Spanish Journal of Palaeontology 39, 2024
https://doi.org/10.7203/sjp.28426
Sociedad Española de Paleontología ISSN 2255-0550 / eISSN 2660-9568

OPEN ACCESS RESEARCH PAPER

Taphonomy and palaeoenvironmental interpretation of a new amber-bearing outcrop from the mid-Cretaceous of the Maestrazgo Basin (E Iberian Peninsula)

Tafonomía e interpretación paleoambiental de un nuevo yacimiento de ámbar del Cretácico medio de la Cuenca del Maestrazgo (este de la península ibérica)

Sergio ÁLVAREZ-PARRA, Carlos A. BUENO-CEBOLLADA, Eduardo BARRÓN, Jordi PÉREZ-CANO, María Victoria PAREDES-ALIAGA, Cristóbal RUBIO, Ana RODRIGO, Nieves MELÉNDEZ, Xavier DELCLÒS & Enrique PEÑALVER

Abstract: Cretaceous amber-bearing outcrops are numerous and mainly distributed along the Northern Hemisphere. They have been related to extensive resin mass production occurring from the Barremian to the Campanian presumably due to interrelated abiotic and biotic factors. Amber outcrops are also abundant in the Iberian Peninsula, and they are mostly dated as Albian. Here, we present a new amber-bearing outcrop from the Cretaceous of the Maestrazgo Basin called La Dehesa (Estercuel, Aragón, Spain). This locality is assigned to the Boundary Marls Unit and is known for its rich and diverse palaeobotanical record. The dating of the amber-bearing bed is late Albian–early Cenomanian, based on palynomorphs and ostracods. Amber characteristics are compatible with a medium to long-distance transport before resin deposition, *i.e.*, allochthonous origin. Organism-resin interactions have been identified, such as hyphae of resinicolous fungus in the cortex of the amber, a pholadid boring determined as *Teredolites clavatus*, and an oyster shell that grew on the solidified resin surface. No bioinclusions have been found so far. The study of the microfossils, some of them containing pyrite aggregates or crystals, found in the amber-bearing bed (palynomorphs, plant remains, foraminifers, echinoid spines, ostracods, and vertebrate remains) points to a coastal to inner mixed platform environment.

Resumen: Los yacimientos de ámbar del Cretácico son numerosos y están distribuidos principalmente por el hemisferio norte. Se han relacionado con una producción en masa de resina que ocurrió desde el Barremiense hasta el Campaniense posiblemente debido a la interrelación de factores abióticos y bióticos. Los yacimientos de ámbar también son abundantes en la península ibérica, y son en su mayoría atribuidos al Albiense. Aquí presentamos un nuevo yacimiento de ámbar del Cretácico de la Cuenca del Maestrazgo denominado La Dehesa (Estercuel, Aragón, España). Esta localidad se incluye en la Unidad Margas de Transición y es conocida por su rico y diverso registro paleobotánico. La datación del nivel con ámbar indica una edad Albiense superior–Cenomaniense inferior, a partir de palinomorfos y ostrácodos. Las características del ámbar son compatibles con un transporte de media-larga distancia antes del depósito de la resina, es decir, con un origen alóctono. Se han identificado interacciones organismos-resina tales como hifas de hongo resinícola en la corteza del ámbar, una perforación de foládido identificada como *Teredolites clavatus* y una concha de ostreido que creció en la superficie de resina solidificada. Por el momento no se han hallado bioinclusiones. El estudio de los microfósiles, algunos de ellos con agregados o cristales de pirita, encontrados en el nivel con ámbar (palinomorfos, restos de plantas, foraminíferos, espinas de erizo, ostrácodos y restos de vertebrados) indica un ambiente marino costero o de plataforma interna mixta.

Received: 26 November 2023
Accepted: 10 March 2024
Published: 15 March 2024

Corresponding author:
Sergio Álvarez-Parra
sergio.alvarez-parra@ub.edu

Keywords:
Fossil resin
Allochthony
Microfossils
Mesozoic
Marine environment
Palaeoecology

Palabras-clave:
Resina fósil
Aloctonía
Microfósiles
Mesozoico
Ambiente marino
Paleoecología

INTRODUCTION

Resins are substances secreted by some gymnosperm and angiosperm plants with a complex composition, including volatile and non-volatile terpenoids, phenols, acids, and other compounds (Langenheim, 1969, 2003; Grimaldi, 2019). Traditionally, it is considered that the resin is a defensive and protective substance whose massive production occurs under one, or a combination, of stressful environmental conditions, which could be both of abiotic (temperature, precipitation, atmospheric gas composition, wildfires, volcanism, changes in sea level, etc.) and biotic origin (damage by arthropods or other animals, and microbial activity) (Langenheim, 1969, 2003; Martínez-Delclòs *et al.*, 2004; Seyfullah *et al.*, 2018; Delclòs *et al.*, 2023). Resins sometimes

trap organisms, which pass to be called bioinclusions (Martínez-Delclòs *et al*., 2004). The possibility of trapping organisms by resins depends on characteristics of the resin, such as production in aerial parts of the trees or the roots, viscosity, and time of hardening, and on characteristics of the same organisms, such as their body size, attraction or repulsion to resin smell, and habitat in the resiniferous forest (Martínez-Delclòs *et al*., 2004; Solórzano-Kraemer *et al*., 2018).

The resin fossilisation process is called amberisation (Martínez-Delclòs *et al*., 2004) and starts when resin flows outside the tree and is in contact with atmospheric gases. Polymerisation of the resin compounds causes its hardening (Langenheim, 2003; Solórzano-Kraemer *et al*., 2020). The resin produced in the aerial parts of the trees, namely trunk and branches, falls gravitationally to the forest litter, and it is superficially buried (Martínez-Delclòs *et al*., 2004). The resin produced by roots rests in the soil and can be affected by resinicolous fungus. Generally, resin from the roots and aerial parts of the trees is transported by runoff to transitional environments, such as deltas or coastal marshes, where its final burial takes place (Martínez-Delclòs *et al*., 2004). From the point of view of the possible resin transport, most amber deposits are considered parautochthonous or allochthonous (Martínez-Delclòs *et al*., 2004; Seyfullah *et al*., 2018). Some amber deposits (autochthonous-parautochthonous) have been identified where the resin pieces were mostly buried in the same place where they formed, without being moved by water transport (Seyfullah *et al*., 2018; Álvarez-Parra *et al*., 2021). The resulting amber pieces are classified as kidney-shaped or root amber, related to the resin produced in the roots, and as aerial amber, related to the resin produced in the trunk and branches (Álvarez-Parra *et al*., 2021).

The oldest known fossil resins date back to the Carboniferous (Bray & Anderson, 2009), and the oldest amber with bioinclusions is from the Triassic (Schmidt *et al*., 2012). However, amber deposits and amber pieces with bioinclusions become abundant and widely distributed since the Barremian, in the Cretaceous period (Delclòs *et al*., 2023). Resin mass production related to conifers occurred during a time range of 54 million years from the Barremian to the Campanian called 'Cretaceous Resinous Interval', presumably due to a combination of abiotic and biotic factors, which are currently under study (Delclòs *et al*., 2023). Cretaceous amber-bearing outcrops are mostly distributed to the Northern Hemisphere, and the most studied deposits are relegated to a few regions, such as western Canada, eastern USA, northeast Spain, western France, Lebanon, Taimyr Peninsula in Russia, and Myanmar (Martínez-Delclòs *et al*., 2004; Seyfullah *et al*., 2018; Delclòs *et al*., 2023). Some Cenozoic ambers, mainly from the Eocene and Miocene, are known to be rich in bioinclusions (Penney, 2010; Solórzano-Kraemer *et al*., 2020; Wang *et al*., 2021).

Most of the amber outcrops in the Iberian Peninsula have been dated as Early Cretaceous, but there are a few ambers related to Triassic, Upper Cretaceous, and Miocene deposits (Delclòs *et al*., 2007; Peñalver & Delclòs, 2010). Cretaceous amber outcrops in the Iberian Peninsula mainly correspond to the western (Lusitanian Basin), northern (Central Asturian Depression and Basque-Cantabrian Basin), and eastern (Maestrazgo Basin) coasts of the palaeoisland of Iberia (Peñalver & Delclòs, 2010). These deposits have been interpreted as transitional environments, including deltas, estuaries, or coastal marshes, where the resin pieces accumulated after a short transport, relating the deposits to parautochthonous amber accumulations (Delclòs *et al*., 2007; Peñalver & Delclòs, 2010). During the mid-Cretaceous, Iberia was located at low latitudes of 25–30ºN under a subtropical-tropical climate along with the development of arid environments at a regional level (Heimhofer *et al*., 2012; Bueno-Cebollada *et al*., 2021, 2023; Barrón *et al*., 2023; Burgener *et al*., 2023). Bioinclusions have been found in ambers from 12 outcrops in the Iberian Peninsula so far (Álvarez-Parra *et al*., 2023, fig. 1). The most studied amber-bearing outcrops are Ariño, El Soplao, Peñacerrada I and II, and San Just (Peñalver & Delclòs, 2010; Álvarez-Parra *et al*., 2021). Regarding the Maestrazgo Basin, bioinclusions have been found in ambers from four outcrops related to the Escucha Formation and Utrillas Group (Peñalver & Delclòs, 2010; Álvarez-Parra *et al*., 2021; Barrón *et al*., 2023; Solórzano-Kraemer *et al*., 2023): Ariño (early Albian), San Just (late Albian), Arroyo de la Pascueta (late Albian), and La Hoya (earliest Cenomanian).

Here, we present a new amber-bearing outcrop from the Cretaceous of the Maestrazgo Basin called La Dehesa, in Estercuel (Teruel, Aragón, Spain). This palaeontological locality is assigned to the Boundary Marls Unit, latest Albian–earliest Cenomanian in age (Villanueva-Amadoz *et al*., 2011), and is known for its palaeobotanical record previously studied (*e.g.*, Sender *et al*., 2012; Santos *et al*., 2023). We focus on the characteristics and taphonomy of the amber and the associated fossil record to interpret the palaeoenvironment of the original resin deposition.

GEOLOGICAL SETTING

The Iberian Range (Fig. 1A) is an intraplate chain that resulted from the tectonic inversion of the Mesozoic Iberian Basin Rift System (**IBRS**) during the Alpine orogeny in the Cenozoic (Sopeña *et al*., 2004; De Vicente *et al*., 2009; Vergés *et al*., 2019). The IBRS is structured in five sedimentary basins (Valencia, Cuenca, Cameros, Central Iberian, and Maestrazgo), and its evolution comprises two rifting stages with their respective post-rift phases. The first rifting stage spanned Permian–latest Triassic, and was followed by an Early to Middle Jurassic post-rift phase (Sopeña *et al*., 2004; López-Gómez *et al*., 2019; Gómez *et al*.,

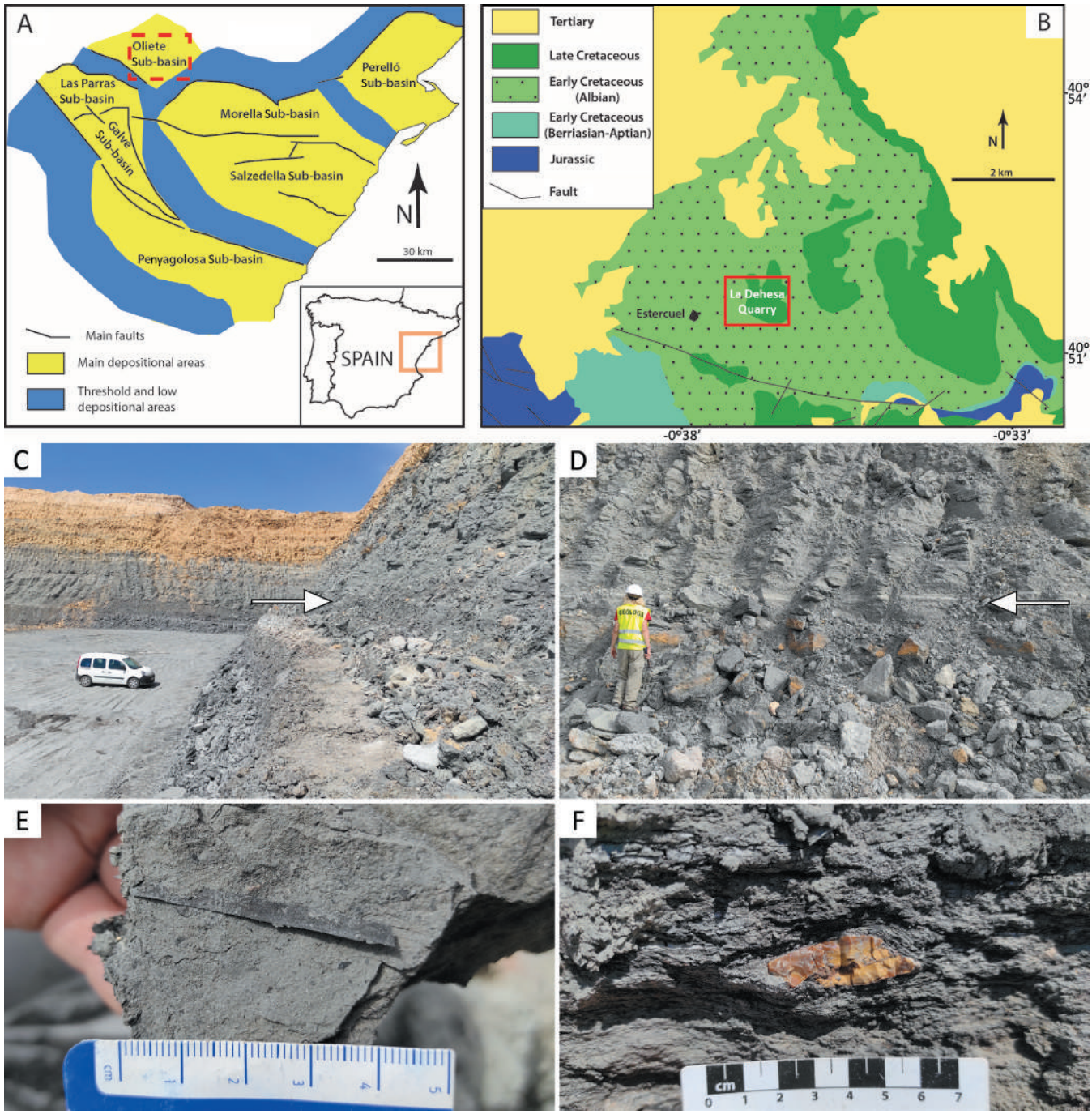

Figure 1. Geological setting of the La Dehesa locality (late Albian–early Cenomanian; Estercuel, Aragón, Spain). **A,** Map of the Maestrazgo Basin indicating the study area in Oliete Sub-basin, modified from Barrón *et al*. (2023) after Aurell *et al*. (2016); **B,** geological map of the study area showing the location of the La Dehesa Quarry, modified from the Magna IGME 1: 50,000 nº 493 (Almela *et al*., 1975); **C**–**D,** photographs of the succession in the La Dehesa Quarry indicating the studied amber-bearing bed (interval 11) with white arrows; **E,** plant remain; **F,** amber piece in the rock matrix.

2019), and the second lasted from the Late Jurassic (Kimmeridgian) to the Early Cretaceous (middle Albian) and was preceded by a Late Cretaceous post-rift phase (Sopeña *et al*., 2004; Aurell *et al*., 2019; Martín-Chivelet *et al*., 2019a, 2019b).

The Maestrazgo Basin is in the eastern sector of the Iberian Ranges. This basin is divided into several sub-basins (Fig. 1A), that were formed during the second rifting stage (Salas *et al*., 2001; Martín-Chivelet *et al*., 2019a, 2019b). The studied locality is in the La Dehesa Quarry (Estercuel municipality, Teruel, Aragón, Spain), in the Oliete Sub-basin, at the northern part of the Maestrazgo Basin (Fig. 1B). The studied sedimentary succession comprises two mid-Cretaceous litho-stratigraphic units: 1) at the base, the Utrillas Group (initially defined with the rank of formation by Aguilar *et al*. (1971), and currently reinterpreted as a group by Rodríguez-López *et al*. (2009)) composed of siliciclastic continental to coastal deposits (Rodríguez-López *et al*., 2012, 2013), and 2) at the top, the Mosqueruela

Formation composed of shallow marine carbonates (Canérot *et al*., 1982). In this regard, the Utrillas Group in the Maestrazgo Basin, described initially as fluvial deposits with tidal influence (Pardo, 1974), has been reinterpreted as deposited in a fore-erg setting where aeolian dunes interacted with tide-dominated coastal deposits giving rise to a wide range of sedimentary environments (Rodríguez-López *et al*., 2009, 2012, 2013). The Utrillas Group is dated as late Albian–earliest Cenomanian in the Maestrazgo Basin based on palinostratigraphy (Barrón *et al*., 2023). While the Mosqueruela Formation is dated as early Cenomanian based on foraminifers (Canérot *et al*., 1982).

The new studied amber-bearing outcrop, the La Dehesa locality (Fig. 1C–1F), is located in the transition between the Utrillas Group and Mosqueruela Formation. Previous works have referred to this interval as the Boundary Marls Unit (Aguilar *et al*., 1971), an informal lithostratigraphic unit dated as latest Albian–earliest Cenomanian in the Aliaga and Oliete sub-basins (Villanueva-Amadoz *et al*., 2011). The Boundary Marls Unit, corresponding to the uppermost part of the Utrillas Group, represents the transition from continental to the shallow marine deposits of the Mosqueruela Formation (Aguilar *et al*., 1971; Villanueva-Amadoz *et al*., 2011).

Additionally, the Early to Late Cretaceous transition is characterised by the highest global sea levels of the Phanerozoic (Haq, 2014), which gave rise to seaways that flooded large continental areas worldwide. Sea-level fluctuations during the mid to Late Cretaceous indicate a eustatic fall at the beginning of the Albian and a progressive eustatic rise (punctuated by minor regressive phases) during Albian that culminated with the eustatic maximum in the Turonian (Haq, 2014), coinciding with thermal maximum during the Cenomanian/Turonian (*e.g.*, Pucéat *et al*., 2003; Forster *et al*., 2007).

The sedimentary record of the Utrillas Group reflects this eustatic rise during the middle to late Albian in the IBRS, which is indicated by its generalised transgressive trend (*i.e.*, Bueno-Cebollada *et al*., 2021, 2022). These eustatic rise conditions progressively led to the sedimentation of the Mosqueruela Formation in the Maestrazgo Basin. In this regard, the Mosqueruela Formation represents most of the transgressive phase of a 2nd order transgressive-regressive (**T-R**) cycle, spanning the latest Albian to the Turonian, which is well represented in the IBRS (Segura *et al*., 2004; Torromé *et al*., 2022).

The La Dehesa locality is known for the abundant and diverse palaeobotanical record as compression fossils yielded from the lower levels of the stratigraphic section of the quarry, including lycopods, ferns, gymnosperms, and terrestrial and aquatic angiosperms (Sender *et al*., 2012, 2019; Villanueva-Amadoz *et al*., 2014). The palynological assemblage previously studied is dominated by gymnosperms and characterised by the presence of diverse angiosperms (Sender *et al*., 2012). Evidence of numerous plant-insect interactions has been identified in both aquatic and terrestrial angiosperm leaves, pointing to the presence of diverse phytophagous insects in the ecosystem (Estévez-Gallardo *et al*., 2017; Santos *et al*., 2023). The palaeobotanical record of the locality was interpreted to be deposited in a fluvial sedimentary environment with marine inputs together with coastal freshwater ponds and marshes (Sender *et al*., 2012).

MATERIAL AND METHODS

The palaeontological monitoring and tracking works at the La Dehesa Quarry that allowed to prospect and obtain the material were carried out under the permissions Expte.: 007/16-17-18-19-20-21-22-2023, Prev.: 001/14.145 of the Aragón Government (Spain). The studied material is deposited at the Museo de Ciencias Naturales de la Universidad de Zaragoza (Zaragoza, Aragón, Spain).

The palynological sample EMD-11.1 was processed following standard palynological techniques (Traverse, 2007) based on acid treatment with HCl and HF. The residues were sieved through 250, 75 and 10 µm-mesh sieves and mounted in glycerine jelly on glass slides. After that, they were covered by transparent glass coverslips and sealed with paraffin. Photographs of palynomorphs were taken with an Olympus BX51 microscope that incorporate a ColorView IIIu camera using a 100X oil immersion objective.

Amber pieces and amber within the rock matrix were collected from interval 11 of La Dehesa stratigraphic log (Fig. 2). Four rock samples (about 2 kg, 0.9 kg, 0.4 kg, and 0.2 kg) from interval 11 were disaggregated in water for one day. Samples were sieved using meshes of 1-, 0.5-, and 0.2-mm aperture. Once they were dried, microfossils were hand-picked using a small brush under Leica Wild M3Z stereomicroscope. Some of the microfossils were treated with ultrasonic cleaning cycles. Scanning Electron Microscopy (**SEM**) imaging of microfossils was carried out using a Quanta 200 electronic microscope that incorporates Energy Dispersive X-ray (**EDX**) analyser at the SEM Unit of the CCiTUB (Universitat de Barcelona); all specimens were sputtered with graphite. The Fourier Transform Infrared Spectroscopy (**FTIR**) analysis of La Dehesa amber was conducted using an IR PerkinElmer Frontier spectrometer with a diamond ATR system, a temperature-stabilised DTGS detector, and a CsI beam splitter at the Molecular Spectrometry Unit of the CCiTUB. FTIR graphic was obtained through R 4.0.4 software. Microphotographs were taken using a Leica Wild M3Z stereomicroscope and an Olympus CX41 compound microscope, both with an attached sCMEX20 digital camera. Possible aerial amber pieces were cut and polished in search of bioinclusions. Figures have been processed using Photoshop CS6.

RESULTS

Sedimentary section and amber-bearing beds description

In the study area, the Boundary Marls Unit is dominated by dark grey mudstones and marlstones, which contain plant remains and root traces at some levels and represent approximately 80% of the thickness of the logged section (Fig. 2). Mudstone and marlstone levels are usually massive. However, heterolithic bedding, mainly wavy and flaser, may also occur. The mudstone/marlstone levels alternate with 100 to 10 cm-thick sandy limestone beds with bivalve shell fragments, which contain percentages up to 20–30% of quartz grains. Limestone beds mainly depict mudstone to wackestone textures; however, they may locally show packstone-grainstone textures (*e.g.*, interval 4 of the logged section; Fig. 2). Regarding their geometry, limestone beds are mostly tabular and laterally continuous across the outcrop; notwithstanding, they may also show lens-shaped bodies extending laterally for 20 to 30 m (*e.g.*, intervals 13 and 14; Fig. 2). Amber-bearing strata are located in intervals 11 and 13 of the studied section (Fig. 2), being interval 11 where the main accumulation of amber occurs. In this interval, amber is associated with mollusc remains (including oysters and other bivalves and gastropods as well). Conversely, amber pieces are found as scattered accumulations in interval 13.

Interval 11 contains framboidal pyrite aggregates and pyrite crystals with octahedral or spherical morphology (Fig. 3). Framboids are composed of tens to hundreds of small octahedral crystals, and the size of a whole structure is up to 15 µm. EDX spectra show abundant concentrations of S and Fe, together with minor amounts of O (Data S1–S3). Scattered octahedral crystals have a diameter of 5 µm and their composition is similar to that observed in the framboids, suggesting that they may have had a similar origin. Thus, octahedrons may correspond to disaggregated or broken pyrite framboids. Spherules have an octahedral-like size, but EDX analyses show higher amounts of S and Fe than the framboids and no O (Data S4).

Amber characteristics

Amber pieces at interval 11 of the section are embedded in a tough rock matrix consisting of mudstones and marlstones (Fig. 4). Most of the amber pieces are found fragmented and they easily disaggregate when extracted from the rock matrix. Their appearance includes yellow and reddish-brown colour, and their size range encompasses from a couple of centimetres to more than ten centimetres. The morphologies of the amber pieces link most of them to a subterranean origin in the roots (Álvarez-Parra *et al*., 2021), *i.e.*, kidney-shaped or root amber pieces. They are irregular in shape (flattened or nearly spherical), showing an external crust, lacking desiccation surfaces, and including whitish layers that might correspond to phloem sap flows similar to those from El Soplao amber (Lozano *et al*., 2020). A few possible aerial amber pieces have been observed (Fig. 4I). No bioinclusions have been found in La Dehesa amber so far.

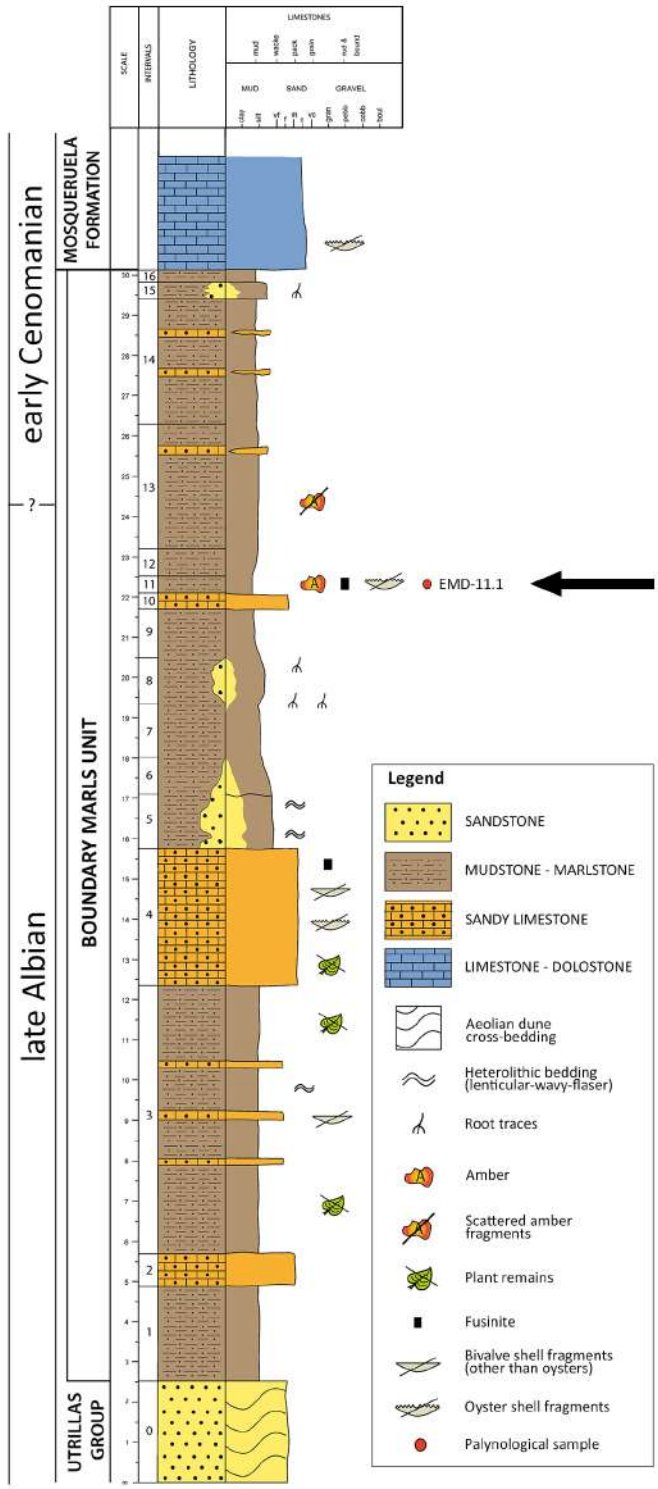

Figure 2. Stratigraphic log of the La Dehesa Quarry in the Maestrazgo Basin (Estercuel, Aragón, Spain) indicating with an arrow the location of the amber-bearing bed studied here (interval 11). Scattered amber pieces were also found at interval 13.

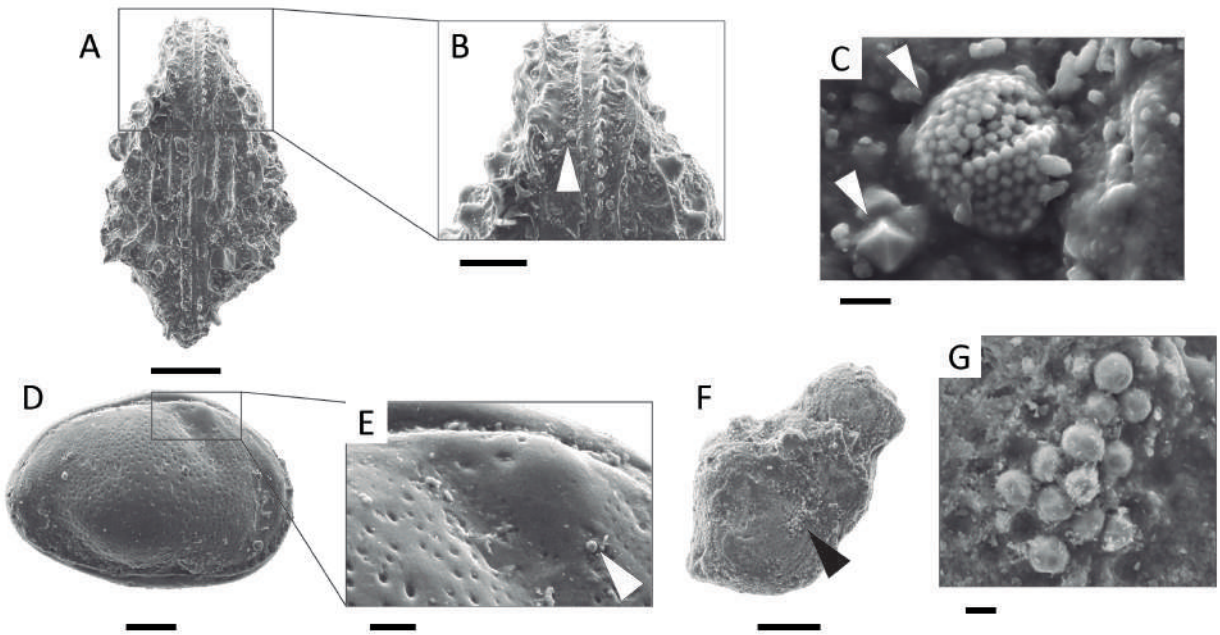

Figure 3. Pyrite framboids found in microfossils from interval 11 of the La Dehesa locality (late Albian–early Cenomanian; Estercuel, Aragón, Spain). **A**–**C,** Framboids and octahedral pyrite found in an ostracod carapace of *Cythereis* (*Rehacythereis*) cf. *pseudobartensteini*, MPZ 2024/32; **D**–**E,** spherical pyrite crystal found on a carapace of *Schuleridea* sp., MPZ 2024/44; **F**–**G,** framboid-like structure formed by spherical pyrite crystals on an echinoid remain, MPZ 2024/25. EDX spectra can be found in Data S1–S4; scale bars = 0.2 mm (A), 0.1 mm (B, D, F), 0.005 mm (C, G), 0.02 mm (E).

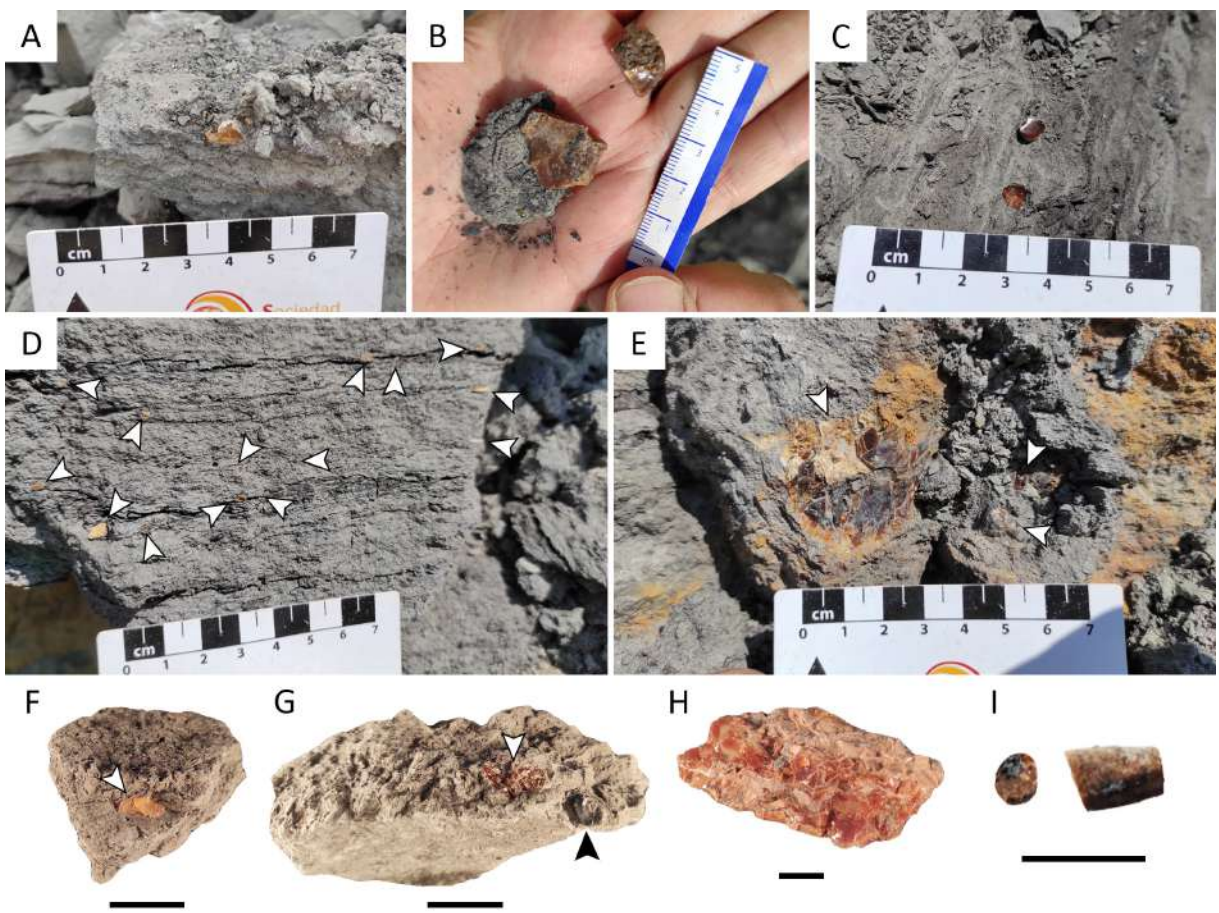

Figure 4. Amber from interval 11 of the La Dehesa locality (late Albian–early Cenomanian; Estercuel, Aragón, Spain). **A**–**C,** Small amber pieces in rock matrix; **D**–**E,** photographs of interval 11 showing abundant millimetric and centimetric amber pieces indicated with white arrowheads; **F,** amber piece in rock matrix, MPZ 2024/09; **G,** amber piece (white arrowhead) very close to an oyster shell (black arrowhead) in rock matrix, MPZ 2024/12 a and MPZ 2024/12 b; **H,** reddish-brown amber piece with whitish outer layer, MPZ 2024/07; **I,** possible aerial amber piece with stalactite-shaped morphology; scale bars = 2 cm (F, G), 1 cm (H, I).

The FTIR spectrum of a transparent amber piece (Fig. 5) shows the characteristics of Cretaceous amber (Grimalt *et al*., 1988; Alonso *et al*., 2000), such as bands at about 2950 cm^{-1} (carbon-hydrogen stretching band), 1700 cm^{-1} (carbonyl band), and 1470 cm^{-1} and 1380 cm^{-1} (bending carbon-hydrogen bands). Hydroxyl bands are present at about 3500 cm^{-1}. Exocyclic methylenic bands are absent at 1640 cm^{-1} and 880 cm^{-1}, indicating a high degree of maturation. The FTIR spectrum from La Dehesa amber has less intense bands, but it does not show significant differences in comparison with the spectra of the other ambers from the Maestrazgo Basin (Peñalver *et al*., 2007; Álvarez-Parra *et al*., 2021; Solórzano-Kraemer *et al*., 2023).

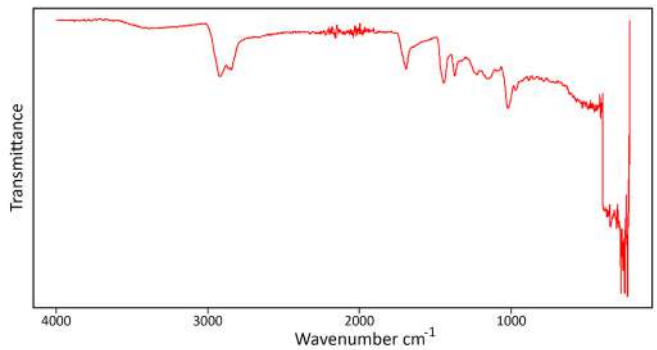

Figure 5. Fourier Transform Infrared Spectroscopy (**FTIR**) spectrum of La Dehesa amber (late Albian–early Cenomanian; Estercuel, Aragón, Spain).

Interestingly, some amber pieces show evidence of interaction between organisms and resin in the palaeoenvironment. The sample MPZ 2024/08 is an amber piece containing a club-shaped (clavate) structure filled with lithified sediment and a connection with the external amber surface (Fig. 6A, 6B). This structure is mostly smooth, but two slightly sigmoidal striations are visible. Other Cretaceous ambers show this kind of structures, which have been identified

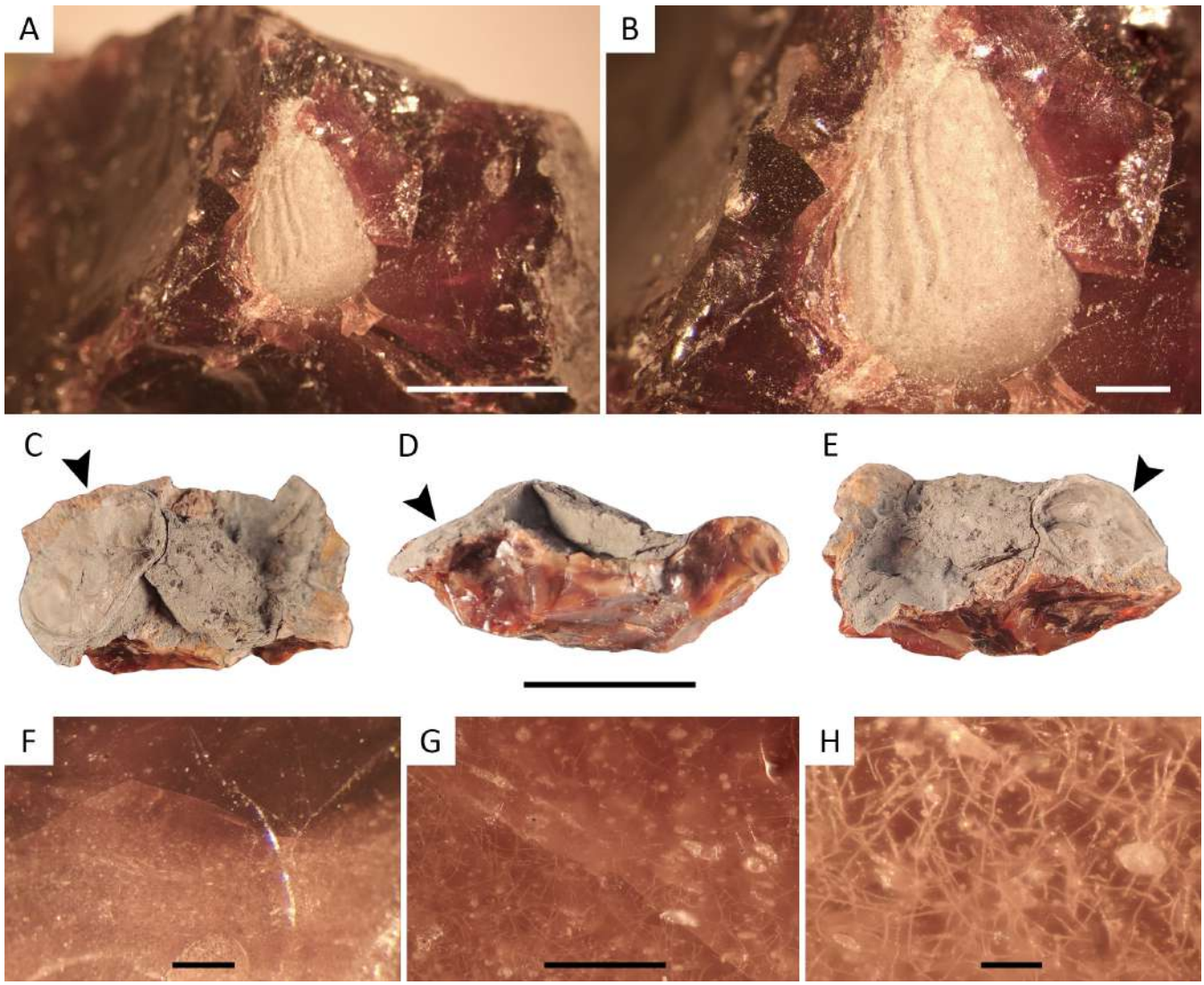

Figure 6. Amber pieces from interval 11 of La Dehesa locality (late Albian–early Cenomanian; Estercuel, Aragón, Spain) showing evidence of interaction between organisms and resin. **A**–**B,** Bivalve pholadid boring in amber piece MPZ 2024/08 identified as *Teredolites clavatus*; **C**–**E,** oyster shell (black arrowhead) that grew on solidified resin, piece MPZ 2024/11 b; **F**–**H,** mycelia of resinicolous fungus in the cortex of amber, piece MPZ 2024/11 a; scale bars = 4 mm (A), 1 mm (B), 2 cm (C–E), 0.5 mm (F), 0.2 mm (G), 0.1 mm (H).

as bivalve borings (Smith & Ross, 2017; Mayoral *et al*., 2020). The specimen in La Dehesa amber has a morphology that can be associated with *Teredolites clavatus*, similar to San Just amber specimens (Mayoral *et al*., 2020). This ichnospecies is related to martesiine (Pholadidae) bivalves (Smith & Ross, 2017). The striations might correspond to movement marks in relation to the rugose ornamentation of the producer (Mayoral *et al*., 2020). The sample MPZ 2024/11 is an amber piece of taphonomic importance, as it shows an oyster shell that grew on the solidified resin surface (Fig. 6C–6E) and networks of mycelia formed by hyphae of resinicolous fungus in the cortex of the amber (Fig. 6F–6H). These two organism-resin interactions have also been described in other Cretaceous ambers (Speranza *et al*., 2015; Mao *et al*., 2018).

Micropalaeontology

Palynomorphs. The palynological study of the sample EMD-11.1 from interval 11 reveals a mixed assemblage comprising marine and terrestrial palynomorphs (Fig. 7; Tab. S1). Most of the specimens of this level belong to the groups: dinoflagellate cysts (10 morphospecies), spores of vascular cryptogams (18 morphospecies), and pollen grains (11 morphospecies). In addition, a few acritarchs, algae and test lining of foraminifers have been identified. Dinoflagellate cysts represent the most abundant group accounting for 57.49% of the identified palynomorph (Fig. 7A–7D). The morphospecies *Oligosphaeridium complex* (Fig. 7A) and *Canningia* cf. *reticulata* (Fig. 7B) are the most conspicuous dinocysts with values of 25.13% and 7.77%, respectively. Lycophyte and fern spores exhibit high diversity but low values, 11.67% (Fig. 7E), being the most relevant the psilate *Cyathidites australis*. Pollen grains of gymnosperms represent 28.24% of the palynomorphs (Fig. 7F–7J), and those attributed to conifers are the most frequent. Grains of the extinct family Cheirolepidiaceae (Fig. 7G) and bisaccate pollen (Fig. 7H) are relevant, showing values of 6.73% and 5.96%, respectively. It is remarkable the abundance of pollen produced by Araucariaceae (13.73%), which is represented by four different morphospecies (*Araucariacites australis*, *Araucariacites* spp., *Balmeiopsis limbata* (Fig. 7I), *Callialasporites dampieri* (Fig. 7J)). Only four grains of angiosperm pollen have been found (Fig. 7K), representing 1.04% of the total identified palynomorphs.

Plant remains. The rock in which amber pieces are found shows abundant plant remains of uncertain affinity (Fig. 1E). Fusinite (charcoal) is abundant in interval 11, associated with the amber, although the poor preservation avoids a taxonomic wood determination (Fig. 8A, 8B). Two fragments of twigs have been found

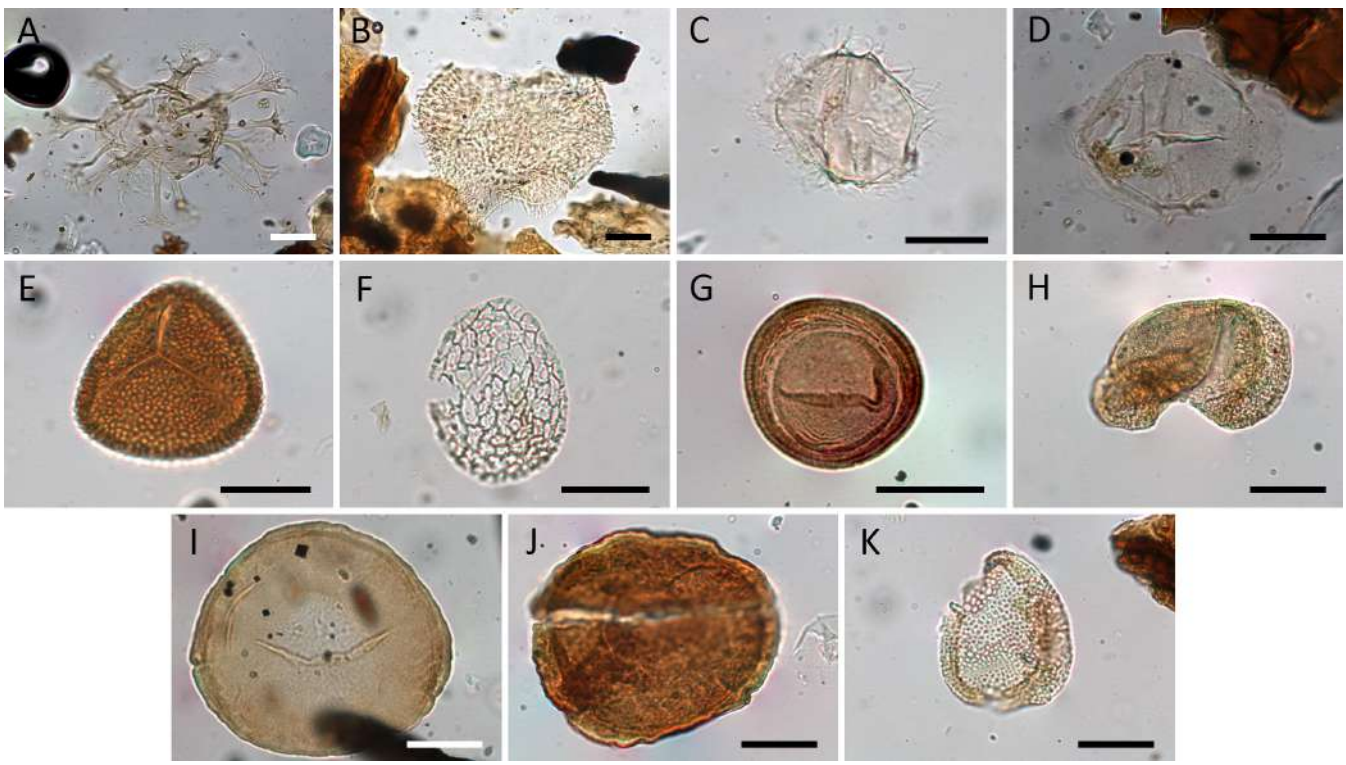

Figure 7. Selected palynomorphs from interval 11 of La Dehesa locality (late Albian–early Cenomanian; Estercuel, Aragón, Spain), present in the palynological sample EMD-11.1. Dinoflagellate: **A**–**D**; Pterydophyta: **E**; Coniferophyta: **F**–**J**; Magnoliophyta: **K**; **A,** *Oligosphaeridium complex*; **B,** *Canningia* cf. *reticulata*; **C,** *Palaeohystrichophora infusorioides*; **D,** *Palaeoperidinium* sp.; **E,** *Microreticulatisporites sacalii*; **F,** *Afropollis jardinus*; **G,** *Classopollis major*; **H,** undetermined bisaccate pollen grain; **I,** *Balmeiopsis limbata*; **J,** *Callialasporites dampieri*; **K,** *Dichastopollenites*? sp.; scale bars = 20 µm. All at the same scale. Full list of palynomorphs from sample EMD-11.1 is available in Table S1.

(Fig. 8C), one corresponding to a middle part, and another corresponding to a distal part. Both are more than 5 mm long. They show homophylly with rounded, alternate leaves, and are tentatively identified as *Pagiophyllum*? sp. (Pinopsida: Araucariaceae), based on the similarity to the twigs of this morphogenus from other Early Cretaceous outcrops in Spain (Barale, 1989; Gómez *et al*., 1999). Interestingly, *Pagiophyllum* sp. twigs previously described from the La Dehesa locality show rhombic leaves with a sharp apex (Sender *et al*., 2012).

Foraminifera. The studied samples from interval 11 have yielded scarce foraminifers represented only by benthic miliolids (Fig. 8D, 8E) and an undetermined benthic

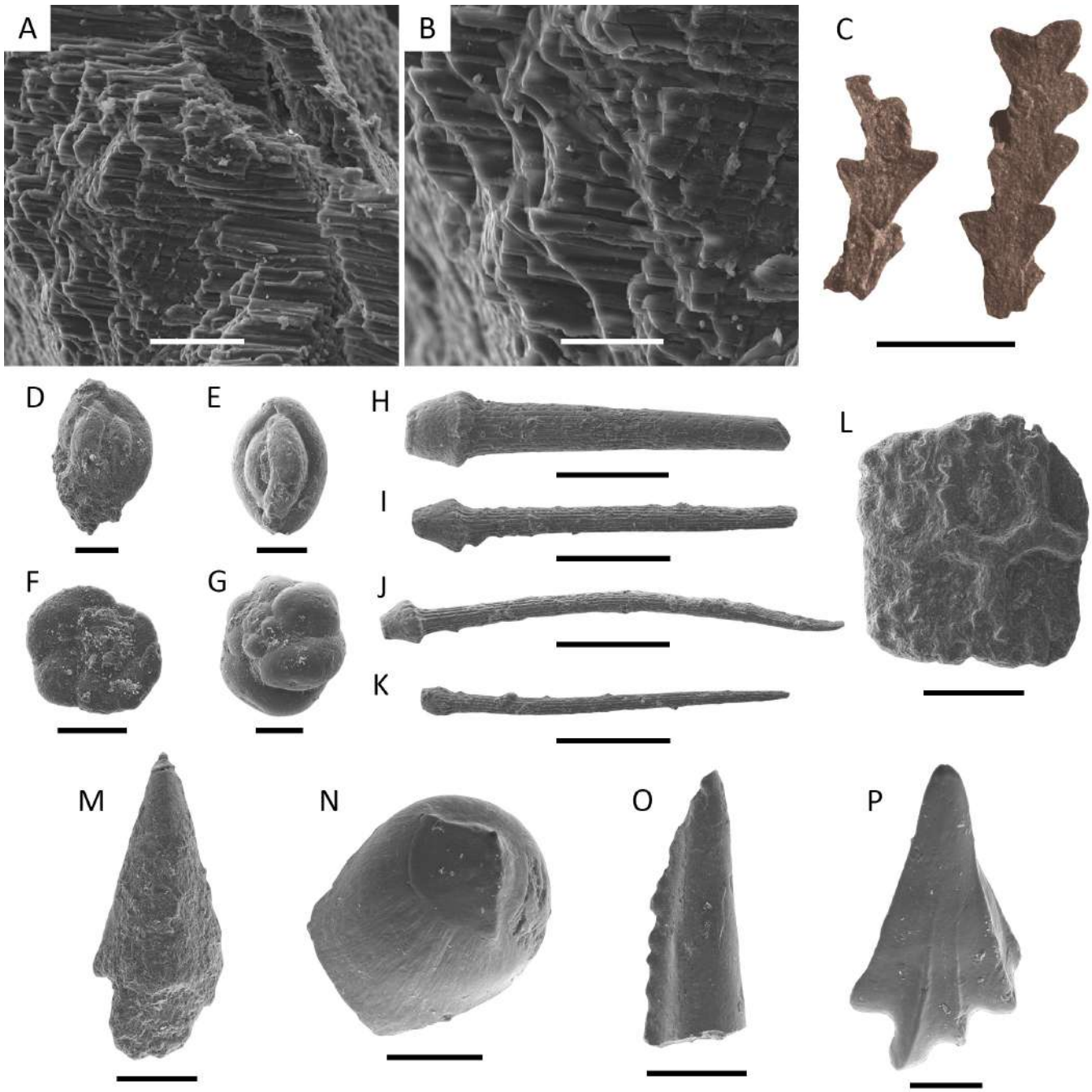

Figure 8. Microfossils from interval 11 of La Dehesa locality (late Albian–early Cenomanian; Estercuel, Aragón, Spain). **A**–**B,** Fusinite (charcoal), B is a detail of A, MPZ 2024/27; **C,** two plant twigs identified as *Pagiophyllum*? sp. (Pinopsida: Araucariaceae), MPZ 2024/10 a and MPZ 2024/10 b; **D**–**E,** benthic miliolid Foraminifera, MPZ 2024/21 and MPZ 2024/24; **F**–**G,** undetermined benthic Foraminifera, MPZ 2024/22 and MPZ 2024/23; **H**–**I,** irregular echinoid spines morphotype 1, MPZ 2024/13 and MPZ 2024/15; **J**–**K,** irregular echinoid spines morphotype 2, MPZ 2024/14 and MPZ 2024/16; **L,** fragment of possible interambulacral plate probably belonging to a regular echinoid, MPZ 2024/26; **M,** conical tooth lacking enameloid of actinopterygian affinity, MPZ 2024/18; **N,** bulbous tooth of actinopterygian affinity, MPZ 2024/20; **O,** partial spine of chondrichthyan affinity, MPZ 2024/17; **P,** dermal denticle of neoselachian (chondrichthyan) affinity, MPZ 2024/19; scale bars = 0.1 mm (A, O), 0.05 mm (B), 5 mm (C), 0.2 mm (D–G, N, P), 1 mm (H–L), 0.5 mm (M).

morphotype (Fig. 8F, 8G). A more precise taxonomic determination is challenging due to the limited number of specimens and their state of preservation.

Ostracods. Twelve morphotypes of ostracod carapaces from interval 11 have been identified and preliminarily determined at genus and/or species levels (Fig. 9). Most of the ostracod specimens belong to *Paracypris* sp. (Candonidae) and *Asciocythere* aff. *compressa* (Schulerideidae). Other, less abundant ostracods are determined as *Cythereis* (*Rehacythereis*) cf. *pseudobartensteini* (Cytheridae), *Cytherella* sp. (Cytherellidae), *Cytheropteron* sp. (Cytheruridae), *Oertiella* sp. (Trachyleberididae), and *Schuleridea jonesiana* (Schulerideidae). Carapaces of all these species are complete, mostly with both valves anatomically attached and without evidence of transport (such as broken specimens or superficial abrasion of the carapaces). Thus, it is evidence of autochthony (*e.g.*, Trabelsi *et al*., 2021). In contrast, carapaces of *Schuleridea* sp. and *Schuleridea alata* show moderate damage (surface abrasion, spines broken), suggesting that most of the specimens suffered a short transport. Carapaces assigned to *Pterygocythereis* cf. *robusta* and *Pterygocythereis* gr. *pulvinata* (Trachyleberididae) are very rare and mostly broken, suggesting transport. The species *Platycythereis degenerata* (Trachyleberididae) is represented only by a few uncompleted and superficially abraded carapaces, suggesting longer transport.

Echinoids. Two morphotypes of isolated echinoid spines from interval 11 have been found. On one hand, thick and straight spines with a longitudinally striate shaft and a prominent base (Fig. 8H, 8I); all spines belonging to this morphotype are incomplete at the tip. On the other hand, thin and slightly curved spines also with a longitudinally striate shaft (Fig. 8J, 8K); most of the spines belonging to this morphotype are complete, being about 3–4 mm long. Based on the short longitude, the slender shape, and the longitudinal striation of the spines, they belonged to irregular echinoids. Furthermore, a fragment of a possible interambulacral plate with polygonal ornamentation, perhaps belonging to a regular echinoid, has also been identified (Fig. 8L).

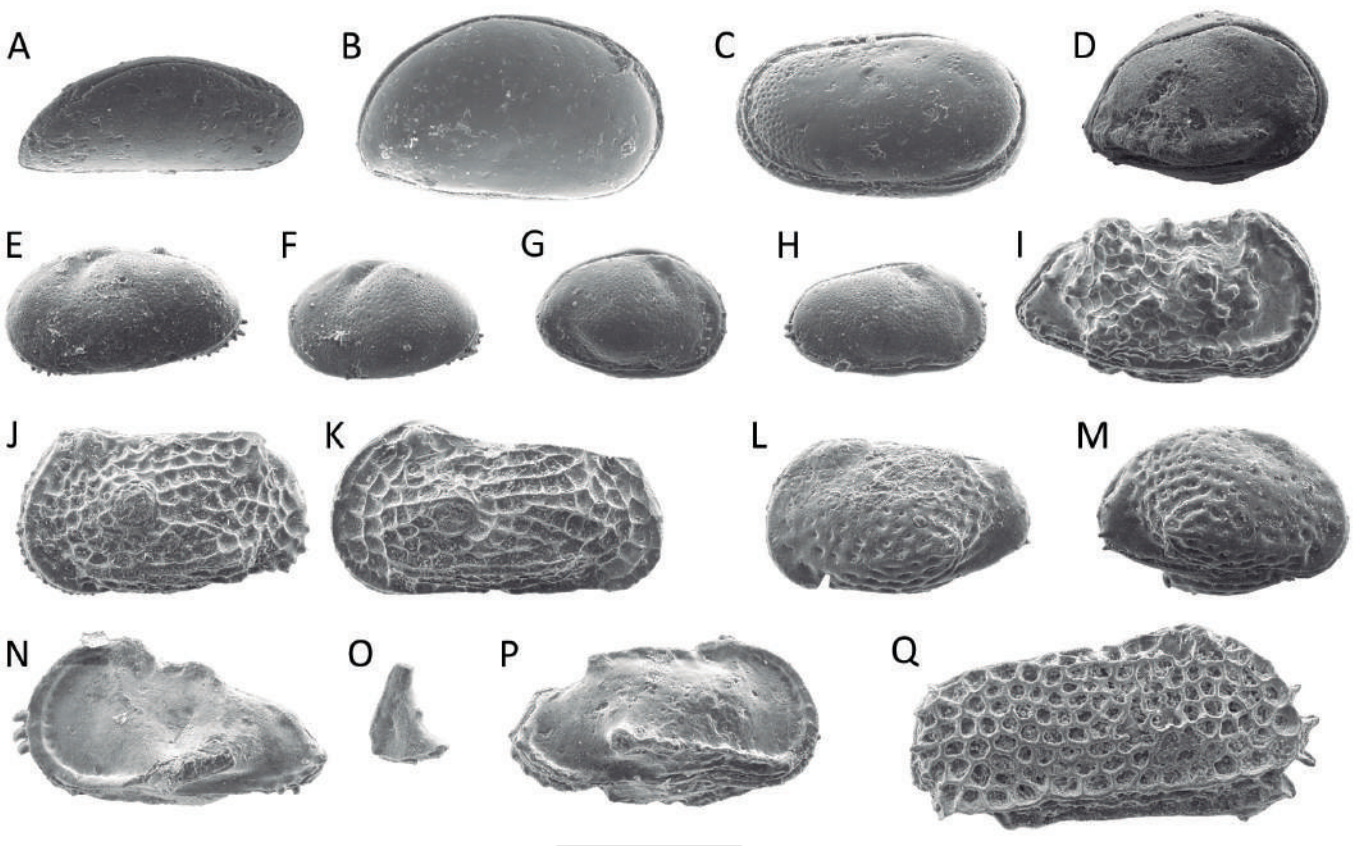

Figure 9. Ostracod carapaces from interval 11 of La Dehesa locality (late Albian–early Cenomanian; Estercuel, Aragón, Spain). **A,** *Paracypris* sp., MPZ 2024/28; **B,** *Asciocythere* aff. *compressa*, MPZ 2024/29; **C,** *Cytherella* sp., MPZ 2024/30; **D,** *Schuleridea alata*, MPZ 2024/46; **E**–**F,** *Schuleridea jonesiana*, male and female carapace respectively, MPZ 2024/41 and MPZ 2024/43; **G**–**H,** *Schuleridea* sp., male and female carapace respectively, MPZ 2024/44 and MPZ 2024/42; **I,** *Cythereis* (*Rehacythereis*) cf. *pseudobartensteini*, MPZ 2024/33; **J**–**K,** *Oertiella* sp., male and female carapace respectively, MPZ 2024/39 and MPZ 2024/36; **L**–**M,** *Cytheropteron* sp., male and female carapace respectively, MPZ 2024/38 and MPZ 2024/40; **N**–**O,** *Pterygocythereis* cf. *robusta*, fragment in O was broken during the preparation of the SEM stub, MPZ 2024/34; **P,** *Pterygocythereis* gr. *pulvinata*, MPZ 2024/35; **Q,** *Platycythereis degenerata*, MPZ 2024/37. All at the same scale; scale bar = 0.5 mm.

Vertebrates. Fish remains from interval 11 have been identified as belonging to chondrichthyans (*i.e.*, cartilaginous fishes) and actinopterygians (*i.e.*, ray-finned fishes). Actinopterygian remains correspond to a conical tooth lacking enameloid (Fig. 8M) and a bulbous tooth presenting well-preserved ornamentation at the base (Fig. 8N). Regarding chondrichthyans remains, a partial spine (Fig. 8O) and a dermal denticle of neoselachian affinity (Fig. 8P) have been identified. The dermal denticle possesses an arrow-shaped outline with an anterior extension and two posterior extensions, where two rings are displayed; the base is not well preserved and protrudes laterally below the wings. Although some authors have classified dermal denticles at family or genus levels (*e.g.*, Cappetta, 1987; Thies, 1995), the great morphological and functional disparity of dermal denticles results in a limited taxonomic and systematic value.

DISCUSSION

Age of the amber from the La Dehesa locality

A late Albian age for interval 11 of the La Dehesa locality is suggested by the presence of the dinocyst *Palaeohystrichophora infusorioides*. The oldest occurrences of this morphospecies in southern Europe are recorded in the *Stoliczkaia dispar* ammonite Zone (Foucher & Monteil, 1998), present-day equivalent to the *Mortoniceras fallax*, *M. rostratum*, *M. periflatum*, and *M. briacensis* biozones (Gale *et al*., 2011; Reboulet *et al*., 2014), which corresponds to the Vraconian ("latest" Albian) (Davey & Verdier, 1973). The previous Iberian late Albian records of *P. infusorioides* correspond to marine environments of the Bay of Biscay (Davey, 1979) and Portugal (Berthou & Hasenboehler, 1982), and those coastal environments of the amber-bearing outcrops of Peñacerrada I and II (Barrón *et al*., 2015). A late Albian age is also supported by the occurrence of the ostracod species *Platycythereis degenerata*, which is found in the late Albian of the Basque-Cantabrian Basin and other localities from the Iberian Ranges (López-Horgue *et al*., 1999; Schudack & Schudack, 2009). However, a late Albian–Cenomanian age is supported by the presence of the morphospecies *Microreticulatisporites sacalii*, which appears in strata of that age in Europe and North America (Ravn, 1986; Ludvigson *et al*., 2010). In addition, the occurrence of angiospermous pollen grains similar to those described as *Dichastopollenites*? sp. 1 in the amber-bearing outcrops of Charentes in France (Peyrot *et al*., 2019a) also relates the studied assemblage to the early Cenomanian. The studied ostracod assemblage supports a Cenomanian age by the species *Pterygocythereis* gr. *pulvinata* and *Pterygocythereis* cf. *robusta*. The stratigraphic range of *P*. gr. *pulvinata* is Cenomanian–Turonian (López-Horgue *et al*., 1999). Similarly, *P. robusta* is reported from the Turonian of England, and its oldest occurrence could be Cenomanian (Slipper, 2021). Other species, such as *Schuleridea jonesiana*, have a long biostratigraphic range from the Aptian to the Cenomanian, according to Babinot *et al*. (2007).

Amber-bearing beds of the La Dehesa locality are limited in its top by the occurrence of Cenomanian praealveolinid assemblages in rock corresponding to the overlying Mosqueruela Formation (Canérot *et al*., 1982). We assign the amber from interval 11 of the La Dehesa locality to a late Albian–early Cenomanian age. In comparison, the palaeobotanical remains studied previously were dated as late Albian (Sender *et al*., 2012). These remains were obtained from lower levels in the stratigraphic section of the quarry; therefore, their age is compatible with our dating.

Resiniferous forest and amber taphonomy

The vegetation of the terrestrial areas was probably analogous to that of the late Albian environments inferred for the Maestrazgo Basin, mainly composed of ferns and angiosperms in humid places, conifers in coastal areas, arid woodlands, and salt marshes (Barrón *et al*., 2023). The FTIR spectrum of La Dehesa amber shows similar characteristics to spectra of other ambers from the Maestrazgo Basin (Peñalver *et al*., 2007; Álvarez-Parra *et al*., 2021; Solórzano-Kraemer *et al*., 2023), pointing to similar resin-producing trees (Araucariaceae) and diagenetic conditions, although a gas chromatography-mass spectrometry analysis is required to link the amber with a resin source.

According to Abbink *et al*. (2004), a high percentage of Mesozoic Araucariaceae pollen might be related to plants that grew near seashores. However, extant Araucariaceae species have pollen that does not disperse easily (Peyrot *et al*., 2019b), and various researchers have observed that in modern palynological assemblages from araucarian forests, there are relatively low percentages of Araucariaceae pollen, typically <5–10% (Elliot, 1999). The inferred percentage of araucarian pollen in the sample we studied, which is 13.73%, is notably higher than those found in modern samples. Given this, along with the likelihood that the species producing this pollen may have lived in coastal areas, it is possible that araucarian forests had a significant presence along the coasts during the deposition of interval 11 at the La Dehesa locality.

The occurrence of pyrite crystals in interval 11 is interpreted as a descriptor of redox conditions (Wilkin *et al*., 1996; Schoonen, 2004). According to the size of the crystals (Bond & Wignall, 2010) and the abundance of pyrite crystals and framboid aggregates in the studied samples, lower dysoxic conditions are inferred. Oxygen-available conditions are supported by the occurrence of bioturbation and the abundance of ostracods in interval 11. Occurrence of pyrite is frequent in both empty inner spaces and the surface of amber pieces and fusinised plant remains (*e.g.*,

Alonso *et al*., 2000; Najarro *et al*., 2010; Álvarez-Parra *et al*., 2021). However, it is not possible to confirm if lower dysoxic conditions are common for all amber-bearing deposits or only the ones related to a marine sedimentary environment, and if this type of condition has prime importance for the preservation of amber and other organic components.

Amber pieces show characteristics of resin transport (Martínez-Delclòs *et al*., 2004; Seyfullah *et al*., 2018). They appear fragmented, and their morphology is irregular but lacking delicate protrusions. Root amber pieces are found mixed with pieces of possible aerial origin. Therefore, based on amber characteristics and sedimentology of the amber-bearing interval 11, we infer an allochthonous nature from the amber pieces of the La Dehesa locality. Resin-producing trees were probably placed in coastal areas, as inferred from other amber-bearing outcrops (Barrón *et al*., 2023), and the resulting resin pieces underwent medium-long transport before deposition. However, the presence of networks of mycelia formed by hyphae of resinicolous fungus in the most external layer of the amber indicates that non-solidified resin pieces remained in the forest soil for a certain time before transport (Speranza *et al*., 2015). Interestingly, evidence of resinicolous fungi has not been found in the early Albian Ariño amber (Álvarez-Parra *et al*., 2021). It is possible that this kind of fungus-resin interaction originated along the Albian or depended on the environmental conditions of the forest soil. The abundance of fusinite indicates the development of palaeofires in the resiniferous forest (Sender *et al*., 2015), which in turn could have stimulated resin mass production (Delclòs *et al*., 2023).

Palaeoenvironmental interpretation

According to Davey and Rogers (1975) and McCarthy and Mudie (1998), high abundance and diversity of dinoflagellate cysts, as in the studied assemblage (Tab. S1), indicate open marine depositional settings. Therefore, the miospores are allochthonous in the assemblage. Nearshore depositional conditions are indicated by the percentages of wind-transported pollen belonging to the conifer family Araucariaceae, which is represented by *Araucariacites*, *Balmeiopsis,* and *Callialasporites* (Tab. S1). A marine origin of interval 11 is supported by the dominance of the ostracod genera *Paracypris*, *Cythereis*, and *Pterygocythereis*, which have been related to marine settings in Cretaceous deposits (*e.g.*, López-Horgue *et al*., 1999; Andreu & Bilotte, 2006; Trabelsi *et al*., 2021). In contrast, the genus *Asciocythere* could have also colonised more coastal and salinity-changing intertidal areas, as it has been found associated with charophytes and freshwater ostracods of the genus *Cypridea* in the late Barremian of Lebanon (Sanjuan *et al*., 2021). Records of *Asciocythere* in Albian deposits are related to marine conditions (Cséfán & Tóth, 2018). Benthic miliolids are typical inhabitants of shallow marine and brackish settings near the coastline or transitional environments (Haynes, 1981). However, the scarce number of foraminifers cannot provide accurate palaeoecological information. The finding of oysters and other molluscs is compatible with this interpretation, as they are usually present in coastal environments.

The abundance of echinoid spines and a few marine vertebrate remains also clearly points out a coastal marine sedimentary environment. The relationship between morphology and function of the squamation in extant sharks (Reif, 1982, 1985) suggests that isolated scales can be useful for palaeoenvironmental and palaeoecological inference (Ferrón *et al*., 2014). The morphology of the neoselachian dermal denticle found in interval 11 allows us to classify it as generalised function, bringing protection against predators, ectoparasites, and mechanical drag (Reif, 1978, 1982, 1985; Raschi & Tabit, 1992). This morphotype is usually present in extant demersal and bentho-demersal sharks that habit on sandy and muddy substrates (Ferrón & Botella, 2017; Ferrón *et al*., 2019).

Pholadid martesiine borings are common in Cretaceous ambers (Mao *et al*., 2018; Smith & Ross, 2017; Mayoral *et al*., 2020). They are usually related to a nearshore setting for the resin-producing trees, as martesiine bivalves require non-solidified resin for producing a boring (Mao *et al*., 2018; Smith & Ross, 2017). Based on the sedimentary interpretation of interval 11 of the La Dehesa locality, it is possible that non-solidified resin pieces were transported to a shallow marine environment where bivalves made borings, coincident with the oxygen-available periods that pyrite framboids indicate. We disagree with the taphonomic model for bivalve borings in amber proposed by Mayoral *et al*. (2020) in which bivalves bored in the wood of living trees, and subsequently, wood decay, and is replaced by resin flows. An oyster shell found directly associated with the surface of an amber piece might indicate that the corresponding resin piece was already externally solidified, as the oyster shell is adapted to the shape of the amber surface and not partly included. Therefore, both solidified and non-solidified resin pieces were exposed in coastal settings for a certain period of time. Based on the above information and evidence, we infer a coastal to inner mixed platform environment for interval 11 of the La Dehesa locality.

Comparison with other amber-bearing outcrops

Several Cretaceous amber outcrops developed in relation to shallow marine conditions have been reported, for example, the upper Albian–lower Cenomanian amber from Archingeay-Les Nouillers in France and the early Cenomanian Hukawng Valley amber from Myanmar (Girard *et al*., 2008; Mao *et al*., 2018). Both ambers contain bioinclusions of marine fauna, such as diatoms, radiolarians, sponge spicules, a foraminifer, and an echinoid spine in French amber (Girard *et al*., 2008), and ostracods and an ammonite

in Burmese amber (Xing *et al*., 2018; Yu *et al*., 2019). Thus, the palaeoenvironmental reconstructions are inferred as resiniferous forests under marine influence, located close to or in a beach, and the amber pieces are considered parautochthonous (Girard *et al*., 2008; Mao *et al*., 2018; Smith & Ross, 2017; Yu *et al*., 2019). Although in the case of the Burmese amber, an estuarine-type environment with both freshwater and marine influence has also been proposed (Bolotov *et al*., 2021). Regarding Spanish amber, El Soplao amber outcrop in Cantabria (northern Spain), middle Albian in age, has been discussed to have at least a slight marine influence based on the occurrence of dinoflagellate cysts, foraminiferan linings, and bivalve and gastropod remains in the amber-bearing bed, and bryozoans and serpulids on the surface of a few amber pieces (Najarro *et al*., 2010). Furthermore, amber pieces from El Soplao show evidence of only little abrasion, pointing to a parautochthonous origin (Najarro *et al*., 2009). Considering this information, the taphonomic and palaeoenvironmental interpretation of La Dehesa amber differs from these cases. An interesting comparison framework might be the Upper Jurassic amber of Cape Mondego in Portugal, whose investigation is in progress, and the preliminary results may also indicate an allochthonous deposition of the resin under shallow marine conditions (Sánchez-García *et al*., 2023), similarly to La Dehesa amber.

CONCLUSIONS AND FUTURE DIRECTIONS

Interval 11 of the La Dehesa locality represents a late Albian–early Cenomanian allochthonous amber site related to resin deposited in a coastal to inner mixed platform environment with variable conditions of oxygen availability. It is the only case with these characteristics among the other amber-bearing outcrops in the Iberian Peninsula to date. This study provides new information about the taphonomic and sedimentary conditions of Cretaceous resin and highlights the relevance of the study of amber outcrops, even if there are no bioinclusions in the amber pieces. However, it is required to delve into the geochemical characteristics of La Dehesa amber to infer the taxonomic assignment of the resin-producing trees. Exploration of fluid inclusions in the amber pieces may provide data about the biology of the resiniferous trees and the environmental conditions of the forest. The finding of aerial amber with bioinclusions would enhance the knowledge of the forest fauna and allow a comparison with those of other Cretaceous ambers. Furthermore, it is planned to expand the study of palynomorphs, ostracods, and foraminifers.

Supplementary information. Table S1 and Data S1–S4 are available at the Spanish Journal of Palaeontology website (https://sepaleontologia.es/spanish-journal-palaeontology/) linked to the corresponding contribution.

Table S1. Full list of palynomorphs from interval 11 of the La Dehesa locality (late Albian–early Cenomanian; Estercuel, Aragón, Spain), present in the palynological sample EMD-11.1.

Data S1–S4. Morphologies of pyrite crystals and framboids on microfossils and their EDX profiles, with the abundance of each element.

Author contributions. SÁ-P conceptualised the study. SÁ-P, CAB-C, EB, CR, AR, NM, and EP participated in fieldwork. CR directed the palaeontological monitoring and tracking works. CAB-C and NM made the stratigraphic log. SÁ-P, EB, JP-C, MVP-A, and EP studied the amber pieces and/or microfossils. SÁ-P carried out the FTIR analysis. SÁ-P and JP-C carried out the SEM imaging. SÁ-P, CAB-C, EB, and JP-C prepared the figures. SÁ-P wrote the first draft of the manuscript with inputs of CAB-C, EB, JP-C, and MVP-A. XD and EP supervised and validated the work. All authors reviewed the manuscript.

Competing interest. The authors declare no competing interests.

Funding. This study has been funded by “Ayudas a la Investigación de la Sociedad Española de Paleontología” AJISEP 2022 to SÁ-P, and by the projects PID2022-137316NB “Cretaceous Resin Interval. Abiotic causes and their paleobotanical and paleoecological implications” (CREI), funded by the Spanish Ministerio de Ciencia, Innovación y Universidades with FEDER funds, and 2021SGR-00349 “Geologia Sedimentària” (AGAUR, Generalitat de Catalunya). The coauthor JP-C has economical support from project IBERINSULA PID2020-113912GB-100 (MCIN/AEI/10.13039/501100011033 and the European Regional Development Fund, ERDF).

Author details. **Sergio Álvarez-Parra**[1,2,3], **Carlos A. Bueno-Cebollada**[4], **Eduardo Barrón**[4], **Jordi Pérez-Cano**[2,3,5,6], **María Victoria Paredes-Aliaga**[7], **Cristóbal Rubio**[8], **Ana Rodrigo**[4], **Nieves Meléndez**[9], **Xavier Delclòs**[2,3], **Enrique Peñalver**[4]. [1]State Key Laboratory of Palaeobiology and Petroleum Stratigraphy, Nanjing Institute of Geology and Palaeontology, Chinese Academy of Sciences, Nanjing 210008, China; sergio@nigpas.ac.cn; [2]Departament de Dinàmica de la Terra i de l’Oceà, Facultat de Ciències de la Terra, Universitat de Barcelona, 08028 Barcelona, Spain; [3]Institut de Recerca de la Biodiversitat (IRBio), Universitat de Barcelona, Barcelona, Spain; sergio.alvarez-parra@ub.edu, jordi_perez-cano@ub.edu, xdelclos@ub.edu; [4]Instituto Geológico y Minero de España, Consejo Superior de Investigaciones Científicas (IGME, CSIC), Madrid, Spain; c.bueno@igme.es, e.barron@igme.es, a.rodrigo@igme.es, e.penalver@igme.es; [5]Institut Català de Paleontologia Miquel Crusafont, Universitat Autònoma de Barcelona, ICTA-ICP Building, Campus de la UAB, E-08193 Cerdanyola del Vallès, Spain; jordi.perez@icp.cat; [6]Departament de Mineralogia, Petrologia i Geologia Aplicada, Facultat de Ciències de la Terra, Universitat de Barcelona-UB, 08028 Barcelona, Spain; [7]Institut Cavanilles de Biodiversitat i Biologia Evolutiva, Universitat de València, 46980 Paterna, Spain; maria.v.paredes@uv.es; [8]PALEOYMAS, Pol. Empresarium, 50720 La Cartuja Baja-Zaragoza, Spain; c.rubio@paleoymas.com; [9]Departamento de Geodinámica, Estratigrafía y Paleontología, Facultad de Ciencias Geológicas, Universidad Complutense de Madrid, 28040 Madrid, Spain; snievesml@geo.ucm.es

Acknowledgements. We are grateful for the corrections and suggestions from two anonymous reviewers that improved the earlier version of the manuscript. We would like to thank SAMCA Group, particularly EuroArce Minería S.A., for collaboration and support during fieldwork in the La Dehesa Quarry. The palaeontological monitoring and tracking works were carried out under the permissions Expte.: 007/16-17-18-19-20-21-22-2023, Prev.: 001/14.145 of the Aragón Government (Spain). We are grateful to Rafael López del Valle for the revision of possible aerial amber pieces in search of bioinclusions, Alejandro Gallardo (Laboratory of Palaeontology-Universitat de Barcelona) for preparing rock samples, Jordi Guillem (Universitat de València) and Carles Ferrández-Cañadell (Universitat de Barcelona) for help on identification of foraminifers, and the technicians at the CCiTUB (Universitat de Barcelona). The coauthor JP-C thank the support of Margarita Salas postdoctoral contract (Spanish Ministry of Universities, "Plan de recuperación, transformación y resiliencia" of Spanish Government and the Next Generation founds from the EU) and CERCA program (Generalitat de Catalunya).

REFERENCES

Abbink, O. A., Van Konijnenburg-Van Cittert, J. H. A., & Visscher, H. (2004). A sporomorph ecogroup model for the Northwest European Jurassic–Lower Cretaceous: concepts and framework. *Geologie en Mijnbouw*, *83*(1), 17–31. doi: 10.1017/S0016774600020436

Aguilar, M. J., Ramírez del Pozo, J., & Riba, O. (1971). Algunas precisiones sobre la sedimentación y paleontología del Cretácico Inferior en la zona de Utrillas-Villarroya de los Pinares. *Estudios Geológicos*, *27*, 497–512.

Almela, A., Mansilla, H., Quintero, I., & Gómez, E. (1975). Mapa Geológico de España 1:50.000, hoja n° 493 (Oliete). IGME, Madrid.

Alonso, J., Arillo, A., Barrón, E., Corral, J. C., Grimalt, J., López, J. F., López, R., Martínez-Delclòs, X., Ortuño, V., Peñalver, E., & Trincão, P. R. (2000). A new fossil resin with biological inclusions in Lower Cretaceous deposits from Álava (northern Spain, Basque-Cantabrian Basin). *Journal of Paleontology, 74*, 158–178. doi: 10.1666/0022-3360(2000)074<0158:ANFRWB>2.0.CO;2

Álvarez-Parra, S., Pérez-de la Fuente, R., Peñalver, E., Barrón, E., Alcalá, L., Pérez-Cano, J., Martín-Closas, C., Trabelsi, K., Meléndez, N., López Del Valle, R., Lozano, R. P., Peris, D., Rodrigo, A., Sarto i Monteys, V., Bueno-Cebollada, C. A., Menor-Salván, C., Philippe, M., Sánchez-García, A., Peña-Kairath, C., Arillo, A., Espílez, E., Mampel, L., & Delclòs, X. (2021). Dinosaur bonebed amber from an original swamp forest soil. *eLife*, *10*, e72477. doi: 10.7554/eLife.72477

Álvarez-Parra, S., Peñalver, E., Nel, A., & Delclòs, X. (2023). Barklice (Insecta: Psocodea) from Early Cretaceous resiniferous forests of Iberia (Spanish amber): New Troctomorpha and a possible Psocomorpha. *Cretaceous Research*, *148*, 105544. doi: 10.1016/j.cretres.2023.105544

Andreu, B., & Bilotte, M. (2006). Upper Cenomanian and Turonian ostracodes from the Eastern sub-Pyrenean zone (Southern Corbières, SE France). Systematics, biostratigraphy, palaeoceology and palaeobiogeography. *Revue de Micropaléontologie*, *49*, 55–73. doi: 10.1016/j.revmic.2005.12.001

Aurell, M., Bádenas, B., Gasca, J. M., Canudo, J. I., Liesa, C. L., Soria, A. R., Moreno-Azanza, M., & Najes, L. (2016). Stratigraphy and evolution of the Galve sub-basin (Spain) in the middle Tithonian–early Barremian: implications for the setting and age of some dinosaur fossil sites. *Cretaceous Research, 65*, 138–162. doi: 10.1016/j.cretres.2016.04.020

Aurell, M., Fregenal-Martínez, M., Bádenas B., Muñoz-García, M. B., Élez, J., Meléndez, N., & De Santisteban, C. (2019). Middle Jurassic–Early Cretaceous tectono-sedimentary evolution of the southwestern Iberian Basin (central Spain): Major palaeogeographical changes in the geotectonic framework of the Western Tethys. *Earth-Science Reviews*, *199*, 102983. doi: 10.1016/j.earscirev.2019.102983

Babinot, F. F., Moullade, M., & Tronchetti, G. (2007). The upper Bedoulian and lower Gargasian Ostracoda of the Aptian stratotype: Taxonomy and biostatigraphic correlation. *Carnets de Géologie*, *CG2007*(A05), 1–35. doi: 10.4267/2042/8877

Barale, G. (1989). Sur trois nouvelles espèces de Coniférales du Crétacé inférieur d'Espagne: intérêts paléoécologiques et stratigraphiques. *Review of Palaeobotany and Palynology*, *61*(3–4), 303–318. doi: 10.1016/0034-6667(89)90036-5

Barrón, E., Peyrot, D., Rodríguez-López, J. P., Meléndez, N., López Del Valle, R., Najarro, M., Rosales, I., & Comas-Rengifo, M. J. (2015). Palynology of Aptian and upper Albian (Lower Cretaceous) amber-bearing outcrops of the southern margin of the Basque-Cantabrian Basin (northern Spain). *Cretaceous Research*, *52*, 292–312.

Barrón, E., Peyrot, D., Bueno-Cebollada, C. A., Kvaček, J., Álvarez-Parra, S., Altolaguirre, Y., & Meléndez, N. (2023). Biodiversity of ecosystems in an arid setting: the late Albian plant communities and associated biota from eastern Iberia. *PLOS ONE*, *18*, e0282178. doi: 10.1371/journal.pone.0282178

Berthou, P.-Y., & Hasenboehler, B. (1982). Les kystes de dinoflagellés de l'Albien et du Cénomanien de la región de Lisbonne (Portugal). Répartition et intérêt stratigraphique. *Cuadernos de Geología Ibérica*, *8*, 761–779.

Bolotov, I. N., Aksenova, O. V., Vikhrev, I. V., Konopleva, E. S., Chapurina, Y. E., & Kondakov, A. V. (2021). A new fossil piddock (Bivalvia: Pholadidae) may indicate estuarine to freshwater environments near Cretaceous amber-producing forests in Myanmar. *Scientific Reports*, *11*(1), 6646. doi: 10.1038/s41598-021-86241-y

Bond, D. P. G, & Wignall, P. B. (2010). Pyrite framboid study of marine Permian–Triassic boundary sections: A complex anoxic event and is relationship to contemporaneous mass extinction. *Geological Society of America Bulletin*, *122*(7–8), 1265–1279. doi: 10.1130/B30042.1

Bray, P. S., & Anderson, K. B. (2009). Identification of Carboniferous (320 million years old) class Ic amber. *Science*, *326*(5949), 132–134. doi: 10.1126/science.1177539

Bueno-Cebollada, C. A., Barrón, E., Peyrot, D., & Meléndez, N. (2021). Palynostratigraphy and palaeoenvironmental evolution of the Aptian to lower Cenomanian succession in the Serranía de Cuenca (Eastern Spain). *Cretaceous Research*, *128*, 104956. doi: 10.1016/j.cretres.2021.104956

Bueno-Cebollada, C. A., Fregenal-Martínez, M., & Meléndez, N. (2022). Along-strike sedimentological variability

and architectural patterns of the transgression of a "mid"-cretaceous braidplain system (Iberian Basin, eastern Spain): A tool for depicting eustatic and tectonic signatures within the framework of a global transgression. *Sedimentary Geology*, *429*, 106082. doi: 10.1016/j.sedgeo.2022.106082

Bueno-Cebollada, C. A., de la Horra, R., Barrenechea, J. F., Meléndez, N., Barrón, E., & Fregenal-Martínez, M. (2023). Mid-Albian to earliest Cenomanian climate cycles indicated by humid paleosols developed within the arid braidplain facies of the Utrillas Group of east-central Spain. *Palaeogeography, Palaeoclimatology, Palaeoecology*, *626*, 111701. doi: 10.1016/j.palaeo.2023.111701

Burgener, L., Hyland, E., Reich, B. J., & Scotese, C. (2023). Cretaceous climates: Mapping paleo-Köppen climatic zones using a Bayesian statistical analysis of lithologic, paleontologic, and geochemical proxies. *Palaeogeography, Palaeoclimatology, Palaeoecology*, *613*, 111373. doi: 10.1016/j.palaeo.2022.111373

Canérot, J., Cugny, P., Pardo, G., Salas, R., & Villena, J. (1982). Ibérica Central-Maestrazgo. In A. García, L. Sánchez de la Torre, V. Pujalte, J. García Mondéjar, J. Rosell, S. Robles, A. Alonso, J. Canérot, L. Vilas, J. A. Vera, & J. Ramírez del Pozo (Eds.), *El Cretácico de España* (pp. 273–344). Universidad Complutense de Madrid y CSIC.

Cappetta, E. (1987). Chondrichthyes II, Mesozoic and Cenozoic Elasmobranchii. In H. P. Schultze (Ed.), *Handbook of Paleoichthyology, Vol. 3B*. Verlag Dr. Friedrich Pfeil.

Cséfán, T., & Tóth, E. (2018). Mid-Cretaceous/Albian (Cretaceous) ostracod assemblage from NW Hungary reflecting deep marine, nearshore and non-marine environments. *Annales de Paléontologie*, *104*, 267–289. doi: 10.1016/j.annpal.2018.09.003

Davey, R. J. (1979). Marine Apto-Albian palynomorphs from Holes 400A and 402A, IPOD Leg 48, northern Bay of Biscay. In L. Montadert, G. D. Roberts, O. de Charpal, & P. Guennoc (Eds.), *Initial reports of the Deep Sea Drilling Project* (pp. 547–577). U.S. Government Printing Office.

Davey, R. J., & Verdier, J.-P. (1973). An investigation of microplankton assemblages from latest Albian (Vraconian) sediments. *Revista Española de Micropaleontología*, *5*(2), 173–212.

Davey, R. A., & Rogers, J. (1975). Palynomorph distribution in recent offshore sediments along two traverses off South West Africa. *Marine Geology*, *18*(4), 213–225. doi: 10.1016/0025-3227(75)90097-3

De Vicente, G., Vegas, R., Muñoz-Martín, A., Van Wees, J. D., Casas-Sáinz, A., Sopeña, A., Sánchez-Moya, Y., Arche, A., López-Gómez, J., Olaiz, A., & Fernández-Lozano, J. (2009). Oblique strain partitioning and transpression on an inverted rift: The Castilian Branch of the Iberian Chain. *Tectonophysics*, *470*, 224–242. doi: 10.1016/j.tecto.2008.11.003

Delclòs, X., Arillo, A., Peñalver, E., Barrón, E., Soriano, C., López Del Valle, R., Bernárdez, E., Corral, C., & Ortuño, V. M. (2007). Fossiliferous amber deposits from the Cretaceous (Albian) of Spain. *Comptes Rendus Palevol*, *6*(1–2), 135–149. doi: 10.1016/j.crpv.2006.09.003

Delclòs, X., Peñalver, E., Barrón, E., Peris, D., Grimaldi, D. A., Holz, M., Labandeira, C. C., Saupe, E. E., Scotese, C. R., Solórzano-Kraemer, M. M., Álvarez-Parra, S., Arillo, A., Azar, D., Cadena, E. A., Dal Corso, J., Kvaček, J., Monleón-Getino, A., Nel, A., Peyrot, D., Bueno-Cebollada, C. A., Gallardo, A., González-Fernández, B., Goula, M., Jaramillo, C., Kania-Kłosok, I., López-Del Valle, R., Lozano, R. P., Meléndez, N., Menor-Salván, C., Peña-Kairath, C., Perrichot, V., Rodrigo, A., Sánchez-García, A., Santer, M., Sarto i Monteys, V., Uhl, D., Viejo, J. L., & Pérez-de la Fuente, R. (2023). Amber and the Cretaceous Resinous Interval. *Earth-Science Reviews*, *243*, 104486. doi: 10.1016/j.earscirev.2023.104486

Elliot, M. B. (1999). Modern pollen–vegetation relationships in Northland, New Zealand. *New Zealand Journal of Botany*, *37*, 131–148. doi: 10.1080/0028825X.1999.9512619

Estévez-Gallardo, P., Sender, L. M., Mayoral, E., & Diez, J. B. (2017). First evidence of insect herbivory on Albian aquatic angiosperms of the NE Iberian Peninsula. *Earth and Environmental Science Transactions of the Royal Society of Edinburgh*, *108*(4), 429–435. doi: 10.1017/S1755691018000555

Ferrón, H. G., & Botella, H. (2017). Squamation and ecology of thelodonts. *PLOS ONE*, *12*, e0172781. doi: 10.1371/journal.pone.017278

Ferrón, H. G., Pla, C., Martínez-Pérez, C., Escudero-Mozo, M. J., & Botella, H. (2014). Morphometric Discriminant Analysis of isolated chondrichthyan scales for palaeoecological inferences: the Middle Triassic of the Iberian Chain (Spain) as a case of study. *Journal of Iberian Geology*, *40*, 87–97. doi: 10.5209/REV_JIGE.2014.V40.N1.44089

Ferrón, H. G., Herráiz, J. L., Botella, H., & Martínez-Pérez, C. (2019). Pre-Messinian ecological diversity of Mediterranean sharks revealed by the study of their dermal denticles. *Spanish Journal of Palaeontology*, *34*(2), 289–298. doi: 10.7203/sjp.34.2.16118

Forster, A., Schouten, S., Baas, M., & Sinninghe Damsté, J. S. (2007). Mid-Cretaceous (Albian–Santonian) sea surface temperature record of the tropical Atlantic Ocean. *Geology*, *35*, 919–922. doi: 10.1130/G23874A.1

Foucher J. C., & Monteil, E. (1998). Cretaceous biochronostratigraphy, Chart 5. In P. -C. De Graciansky, J. Hardenbol, T. Jacquin, & P. R. Vail (Eds.), *Mesozoic and Cenozoic sequence stratigraphy of European basins*. Society of Economic Paleontologists and Mineralogists, Special Publication 60.

Gale, A. S., Bown, P., Caron, M., Crampton, J., Crowhurst, S. J., Kennedy, W. J., Petrizzo, M. R., & Wray, D. S. (2011). The uppermost Middle and Upper Albian succession at the Col de Palluel, Hautes-Alpes, France: An integrated study (ammonites, inoceramid bivalves, planktonic foraminifera, nannofossils, geochemistry, stable oxygen and carbon isotopes, cyclostratigraphy). *Cretaceous Research*, *32*, 59–130. doi: 10.1016/j.cretres.2010.10.004

Girard, V., Schmidt, A. R., Saint Martin, S., Struwe, S., Perrichot, V., Saint Martin, J. P., Grosheny, D., Breton, G., & Néraudeau, D. (2008). Evidence for marine microfossils from amber. *Proceedings of the National Academy of Sciences*, *105*(45), 17426–17429. doi: 10.1073/pnas.0804980105

Gómez, B., Barale, G., Martín-Closas, C., Thévenard, F., & Philippe, M. (1999). Découverte d'une flore à Ginkgoales, Bennettitales et Coniférales dans le Crétacé inférieur de la formation Escucha (Chaîne Ibérique Orientale, Teruel, Espagne). *Neues Jahrbuch für Geologie und Paläontologie, Monatshefte*, *11*, 661–675. doi: 10.1127/njgpm/1999/1999/661

Gómez, J. J., Aguado, R., Azerêdo, A. C., Cortés, J. E., Duarte, L. V., O'Dogherty, L., da Rocha, R. B., & Sandoval, J. (2019). The Late Triassic–Middle Jurassic Passive Margin Stage. In C. Quesada, & J. T. Oliveira (Eds.), *The Geology of Iberia: A Geodynamic Approach* (pp. 113–167). Springer Cham.

Grimaldi, D. A. (2019). Amber. *Current Biology*, *29*(18), R861–R862. doi: 10.1016/j.cub.2019.08.047

Grimalt, J. O., Simoneit, B. R. T., Hatcher, P. G., & Nissenbaum, A. (1988). The molecular composition of ambers. *Organic Geochemistry*, *13*(4–6), 677–690. doi: 10.1016/0146-6380(88)90089-7

Haq, B. U. (2014). Cretaceous eustasy revisited. *Global and Planetary Change*, *113*, 44–58. doi: 10.1016/j.gloplacha.2013.12.007

Haynes, J. R. (1981). *Foraminifera*. Springer.

Heimhofer, U., Hochuli, P. A., Burla, S., Oberli, F., Adatte, T., Dinis, J. L., & Weissert, H. (2012). Climate and vegetation history of western Portugal inferred from Albian near-shore deposits (Galé Formation, Lusitanian Basin). *Geological Magazine*, *149*(6), 1046–1064. doi: 10.1017/S0016756812000118

Langenheim, J. H. (1969). Amber: a botanical inquiry. *Science*, *163*(3872), 1157–1169.

Langenheim, J. H. (2003). *Plant resins: chemistry, evolution, ecology, and ethnobotany*. Timber Press.

López-Gómez, J., Alonso-Azcárate, J., Arche, A., Arribas, J., Fernández, J., Borruel-Abadía, V., Bourquin, S., Cadenas, P., Cuevas, P., De la Horra, R., Díez, J., Escudero-Mozo, M. J., Fernández-Viejo, G., Galán-Abellán, B., Galé, C., Gaspar-Escribano, J., Gisbert Aguilar, J., Gómez-Gras, D., Goy, A., Gretter, N., Heredia, N., Lago, M., Lloret, J., Luque, J., Márquez, L., Márquez-Aliaga, A., Martín-Algarra, A., Martín-Chivelet, J., Martín-González, F., Marzo, M., Mercedes-Martín, R., Ortí, F., Pérez-López, A., Pérez-Valera, F., Pérez-Valera, J. A., Plasencia, P., Ramos, E., Rodríguez-Méndez, L., Ronchi, A., Salas, R., Sánchez-Fernández, D., Sánchez-Moya, Y., Sopeña, A., Suárez-Rodríguez, A., Tubía, J. M., Ubide, T., Valero, B., Vargas, H., & Viseras, C. (2019). Permian–Triassic Rifting Stage. In C. Quesada, & J. T. Oliveira (Eds.), *The Geology of Iberia: A Geodynamic Approach. Volume 3: The Alpine Cycle* (pp. 29–112). Springer Cham.

López-Horgue, M. A., Owen, H. G., Rodríguez-Lázaro, J., Orue-Etxebarria, X., Fernández-Mendiola, P. A., & García-Mondéjar, J. (1999). Late Albian–Early Cenomanian stratigraphic succession near Estella-Lizarra (Navarra, central northern Spain) and interregional correlation. *Cretaceous Research*, *20*, 369–402. doi: 10.1006/cres.1999.0162

Lozano, R. P., Pérez-de la Fuente, R., Barrón, E., Rodrigo, A., Viejo, J. L., & Peñalver, E. (2020). Phloem sap in Cretaceous ambers as abundant double emulsions preserving organic and inorganic residues. *Scientific Reports*, *10*, 9751. doi: 10.1038/s41598-020-66631-4

Ludvigson, G. A., Witzke, B. J., Joeckel, R. M., Ravn, R. L., Phillips, P. L., González, L. A., & Brenner, R. L. (2010). New insights on the sequence stratigraphic architecture of the Dakota Formation in Kansas-Nebraska-Iowa from a decade sponsored research activity. *Current Research in Earth Sciences Bulletin*, *258*(2), 1–35.

Mao, Y., Liang, K., Su, Y., Li, J., Rao, X., Zhang, H., Xia, F., Fu, Y., Cai, C., & Huang, D. (2018). Various amberground marine animals on Burmese amber with discussions on its age. *Palaeoentomology*, *1*(1), 91–103. doi: 10.11646/palaeoentomology.1.1.11

Martín-Chivelet, J., López-Gómez, J., Aguado, R., Arias, C., Arribas, J., Arribas, M. E., Aurell, M., Bádenas, B., Benito, M. I., Bover-Arnal, T., Casas-Sainz, A., Castro, J. M., Coruña, F., de Gea, G. A., Fornós, J. J., Fregenal-Martínez, M., García-Senz, J., Garófano, D., Gelabert, B., Giménez, J., González-Acebrón, L., Guimerà, J., Liesa, C. L., Mas, R., Meléndez, N., Molina, J. M., Muñoz, J. A., Navarrete, R., Nebot, M., Nieto, L. M., Omodeo-Salé, S., Pedrera, A., Peropadre, C., Quijada, I. E., Quijano, M. L., Reolid, M., Robador, A., Rodríguez-López, J. M., Rodríguez-Perea, A., Rosales, I., Ruiz-Ortiz, P. A., Sàbat, F., Salas, R., Soria, A. R., Suárez-González, P., & Vilas, L. (2019a). The Late Jurassic–Early Cretaceous Rifting (Chapter 5). In C. Quesada, & J. T. Oliveira (Eds.), *The Geology of Iberia: A Geodynamic Approach. Volume 3: The Alpine Cycle* (pp. 169–249). Springer Cham.

Martín-Chivelet, J., Floquet, M., García-Senz, J., Callapez, P. M., López-Mir, B., Muñoz, J. A., Barroso-Barcenilla, F., Segura, M., Soares, A. F., Dinis, P. M., Marques, J. F., & Arbués, P. (2019b). Late Cretaceous Post-Rift to Convergence in Iberia (Chapter 7). In C. Quesada, & J. T. Oliveira (Eds.), *The Geology of Iberia: A Geodynamic Approach. Volume 3: The Alpine Cycle* (pp. 285–376). Springer Cham.

Martínez-Delclòs, X., Briggs, D. E., & Peñalver, E. (2004). Taphonomy of insects in carbonates and amber. *Palaeogeography, Palaeoclimatology, Palaeoecology*, *203*(1–2), 19–64. doi: 10.1016/S0031-0182(03)00643-6

Mayoral, E., Santos, A., Vintaned, J. G., Wisshak, M., Neumann, C., Uchman, A., & Nel, A. (2020). Bivalve bioerosion in Cretaceous–Neogene amber around the globe, with implications for the ichnogenera *Teredolites* and *Apectoichnus*. *Palaeogeography, Palaeoclimatology, Palaeoecology*, *538*, 109410. doi: 10.1016/j.palaeo.2019.109410

McCarthy, F. M., & Mudie, P. J. (1998). Oceanic pollen transport and pollen: dinocyst ratios as markers of late Cenozoic sea level change and sediment transport. *Palaeogeography, Palaeoclimatology, Palaeoecology*, 138(1–4), 187–206. doi: 10.1016/S0031-0182(97)00135-1

Najarro, M., Peñalver, E., Rosales, I., Pérez-de la Fuente, R., Daviero-Gómez, V., Gómez, B., & Delclòs, X. (2009). Unusual concentration of Early Albian arthropod-bearing amber in the Basque-Cantabrian Basin (El Soplao, Cantabria, Northern Spain): Palaeoenvironmental and palaeobiological implications. *Geologica Acta*, *7*(3), 363–387. doi: 10.1344/105.000001443

Najarro, M., Peñalver, E., Pérez-de la Fuente, R., Ortega-Blanco, J., Menor-Salván, C., Barrón, E., Soriano, C., Rosales, I., López del Valle, R., Velasco, F., Tornos, F. D., Daviero-Gómez, V., Gómez, B., & Delclòs, X. (2010). Review of the El Soplao amber outcrop, Early Cretaceous of Cantabria, Spain. *Acta Geologica Sinica (English Version)*, *84*(4), 959–976. doi: 10.1111/j.1755-6724.2010.00258.x

Pardo, G. (1974). Nota previa sobre las características litoestratigráficas de las formaciones «Arenas de Utrillas» y «Lignitos de Escucha». *Acta Geológica Hispánica*, *IX*(2), 62–66.

Penney, D. (2010). Dominican amber. In D. Penney (Ed.), *Biodiversity of fossils in amber from the major world deposits* (pp. 22–41). Siri Scientific Press.

Peñalver, E., & Delclòs, X. (2010). Spanish amber. In D. Penney (Ed.), *Biodiversity of fossils in amber from the major world deposits* (pp. 236–270). Siri Scientific Press.

Peñalver, E., Delclòs, X., & Soriano, C. (2007). A new rich amber outcrop with palaeobiological inclusions in the Lower Cretaceous of Spain. *Cretaceous Research*, *28*(5), 791–802. doi: 10.1016/j.cretres.2006.12.004

Peyrot, D., Barrón, E., Polette, F., Batten, D. J., & Néraudeau, D. (2019a). Early Cenomanian palynofloras and inferred resiniferous forests and vegetation types in Charentes (southwestern France). *Cretaceous Research*, *94*, 168–189. doi: 10.1016/j.cretres.2018.10.011

Peyrot, D., Playford, G., Mantle, D. J., Backhouse, J., Milne, L. A., Carpenter, R. J., Foster, C., Mory, A. J., McLoughlin, S., Vitacca, J., Scibiorski, J., Mack, C. L., & Bevan, J. (2019b). The greening of Western Australian landscapes: the Phanerozoic plant record. *Journal of the Royal Society of Western Australia*, *102*, 52–82.

Pucéat, E., Lécuyer, C., Sheppard, S. M. F., Dromart, G., Reboulet, S., & Grandjean, P. (2003). Thermal evolution of Cretaceous Tethyan marine waters inferred from oxygen isotope composition of fish tooth enamels. *Paleoceanography*, *18*, 7.1–7.12. doi: 10.1029/2002PA000823

Raschi, W., & Tabit, C. (1992). Functional aspects of placoid scales: a review and update. *Marine and Freshwater Research*, *43*, 123–147. doi: 10.1071/MF9920123

Ravn, R. L. (1986). *Microreticulatisporites sacalii* (Deák and Combaz) n. comb., a stratigraphically significant miospore from the Cenomanian of the United States. *Journal of Paleontology*, *60*(3), 772–777. doi: 10.1017/S0022336000022290

Reboulet, S., Szives, O., Aguirre-Urreta, B., Barragán, R., Company, M., Idakieva, V., Ivanov, M., Kakavadze, M. V., Moreno-Bedmar, J. A., Sandoval, J., Baraboshki, E. J., Çağlar, M. K., Fõzy, I., González-Arreola, C., Kenjo, S., Lukeneder, A., Raisossadat, S. N., Rawson, P. F., & Tavera, J. M. (2014). Report on the 5th International Meeting of the IUGS Lower Cretaceous Ammonite Working Group, the Kilian Group (Ankara, Turkey, 31st August 2013). *Cretaceous Research*, *50*, 126–137. doi: 10.1016/j.cretres.2014.04.001

Reif, W. E. (1978). Types of morphogenesis of the dermal skeleton in fossil sharks. *Paläontologische Zeitschrift*, *52*, 235–257. doi:10.1007/BF03006733

Reif, W. E. (1982). Morphogenesis and function of the squamation in sharks. *Neues Jahrbuch für Geologie und Paläontologie, Abhandlungen*, *164*, 172–183.

Reif, W. E. (1985). *Squamation and ecology of sharks*. Courier Forschungsinstitut Senckenberg.

Rodríguez-López, J. P., Meléndez, N., Soria, A. R., & De Boer, P. (2009). Reinterpretación estratigráfica y sedimentológica de las Formaciones Escucha y Utrillas de la Cordillera Ibérica. *Revista de la Sociedad Geológica de España*, *22*, 163–219.

Rodríguez-López, J. P., Meléndez, N., De Boer, P. L., & Soria, A. R. (2012). Controls on marine-erg margin cycle variability: aeolian-marine interaction in the mid-Cretaceous Iberian Desert System, Spain. *Sedimentology*, *59*, 466–501. doi: 10.1111/j.1365-3091.2011.01261.x

Rodríguez-López, J. P., Meléndez, N., de Boer, P. L., Soria, A. R., & Liesa, C. L. (2013). Spatial variability of multi-controlled aeolian supersurfaces in central-erg and marine erg-margin systems. *Aeolian Research*, *11*, 141–154. doi: 10.1016/j.aeolia.2013.07.002

Salas, R., Guimerà, J., Mas, R., Martín-Closas, C., Meléndez, A., & Alonso, A. (2001). Evolution of the Mesozoic Central Iberian Rift System and its Cainozoic inversion (Iberian Chain). In P. A. Ziegler, W. Cavazza, A. H. F. Roberston, & S. Crasquin- Soleau (Eds.), *Peri-Tethys Memoir 6: Peri-Tethyan Rift/Wrench Basins and Passive Margins* (pp. 145–186). Mémoires du Muséum National d'Histoire Naturelle.

Sánchez-García, A., Silvério, G., Delclòs, X., Barrón, E., & Peñalver, E. (2023). Ámbar del Jurásico Superior de Cabo Mondego (Portugal). *Libro de Resúmenes de las XXXVIII Jornadas SEP* (p. 4). Valencia.

Sanjuan, J., Ghadban, S. E., & Trabelsi, K. (2021). Microfossils (ostracods and charophytes) from the non-marine Lower Cretaceous of Lebanon: Palaeoecology, biostratigraphy and palaeobiogeography. *Cretaceous Research*, *124*, 104806. doi: 10.1016/j.cretres.2021.104806

Santos, A. A., Sender, L. M., Wappler, T., & Diez, J. B. (2023). Plant–insect interactions on aquatic and terrestrial angiosperms from the latest Albian (Early Cretaceous) of Estercuel (northeastern Spain) and their paleoenvironmental implications. *Plants*, *12*(3), 508. doi: 10.3390/plants12030508

Schmidt, A. R., Jancke, S., Lindquist, E. E., Ragazzi, E., Roghi, G., Nascimbene, P. C., Schmidt, K., Wappler, T., & Grimaldi, D. A. (2012). Arthropods in amber from the Triassic Period. *Proceedings of the National Academy of Sciences*, *109*(37), 14796–14801. doi: 10.1073/pnas.1208464109

Schoonen, M. A. (2004). Mechanisms of sedimentary pyrite formation. *Geological Society of America Special Papers*, *379*, 117–134. doi: 10.1130/0-8137-2379-5.117

Schudack, U., & Schudack, M. (2009). Ostracod biostratigraphy in the Lower Cretaceous of the Iberian chain (eastern Spain). *Journal of Iberian Geology*, *35*(2), 141–168.

Segura, M., García-Hidalgo, J. F., Carenas, B., Gil, J., & García, A. (2004). Evolución paleogeográfica de la Cuenca Ibérica en el Cretácico Superior. *Geogaceta*, *36*, 103–106.

Sender, L. M., Villanueva-Amadoz, U., Diez, J. B., Sánchez-Pellicer, R., Bercovici, A., Pons, D., & Ferrer, J. (2012). A new uppermost Albian flora from Teruel province, northeastern Spain. *Geodiversitas*, *34*(2), 373–397. doi: 10.5252/g2012n2a7

Sender, L. M., Villanueva-Amadoz, U., Pons, D., Diez, J. B., & Ferrer, J. (2015). Singular taphonomic record of a wildfire event from middle Albian deposits of Escucha Formation in northeastern of Spain. *Historical Biology*, *27*(3–4), 442–452. doi: 10.1080/08912963.2014.895827

Sender, L. M., Doyle, J. A., Upchurch Jr, G. R., Villanueva-Amadoz, U., & Diez, J. B. (2019). Leaf and inflorescence evidence for near-basal Araceae and an unexpected diversity of other monocots from the late Early Cretaceous of Spain. *Journal of Systematic Palaeontology*, *17*(15), 1313–1346. doi: 10.1080/14772019.2018.1528999

Seyfullah, L. J., Beimforde, C., Dal Corso, J., Perrichot, V., Rikkinen, J., & Schmidt, A. R. (2018). Production and preservation of resins–past and present. *Biological Reviews*, *93*(3), 1684–1714. doi: 10.1111/brv.12414

Slipper, I. J. (2021). Ostracoda from the Turonian of South-East England Part 2. Cytherocopina. *Monographs of the Palaeontographical Society*, *174*(657), 47–168. doi: 10.1080/02693445.2020.1782044

Smith, R. D., & Ross, A. J. (2017). Amberground pholadid bivalve borings and inclusions in Burmese amber: implications for proximity of resin-producing forests to brackish waters, and the age of the amber. *Earth and Environmental Science Transactions of the Royal Society of Edinburgh*, *107*(2–3), 239–247. doi: 10.1017/S1755691017000287

Solórzano-Kraemer, M. M., Delclòs, X., Clapham, M. E., Arillo, A., Peris, D., Jäger, P., Stebner, F., & Peñalver, E. (2018). Arthropods in modern resins reveal if amber accurately recorded forest arthropod communities. *Proceedings of the National Academy of Sciences*, *115*(26), 6739–6744. doi: 10.1073/pnas.1802138115

Solórzano-Kraemer, M. M., Delclòs, X., Engel, M. S., & Peñalver, E. (2020). A revised definition for copal and its significance for palaeontological and Anthropocene biodiversity-loss studies. *Scientific Reports*, *10*, 19904. doi: 10.1038/s41598-020-76808-6

Solórzano-Kraemer, M. M., Sinclair, B. J., Arillo, A., & Álvarez-Parra, S. (2023). A new genus of dance fly (Diptera: Empidoidea: Hybotidae) from Cretaceous Spanish ambers and introduction to the fossiliferous amber outcrop of La Hoya (Castellón Province, Spain). *PeerJ*, *11*, e14692. doi: 10.7717/peerj.14692

Sopeña, A., Gutiérrez-Marco, J. C., Sánchez-Moya, Y., Gómez, J. J., Mas, R., García, A., & Lago, M. (2004). Cordillera Ibérica y Costero Catalana. In J. A. Vera (Ed.), *Geología de España* (pp. 465–528). Sociedad Geológica de España–Instituto Geológico y Minero de España.

Speranza, M., Ascaso, C., Delclòs, X., & Peñalver, E. (2015). Cretaceous mycelia preserving fungal polysaccharides: taphonomic and paleoecological potential of microorganisms preserved in fossil resins. *Geologica Acta*, *13*(4), 363–385. doi: 10.1344/GeologicaActa2015.13.4.8

Thies, D. (1995). Placoid Scales (Chondrichthyes: Elasmobranchii) from the Late Jurassic (Kimmeridgian) of Northern Germany. *Journal of Vertebrate Paleontology*, *15*(3), 463–481. doi: 10.1080/02724634.1995.10011242

Torromé, D., Aurell, M., & Bádenas, B. (2022). A mud-dominated coastal plain to lagoon with emerged carbonate mudbanks: The imprint of low-amplitude sea level cycles (mid-Upper Cretaceous, South Iberian Ramp). *Sedimentary Geology*, *436*, 106178. doi: 10.1016/j.sedgeo.2022.106178

Trabelsi, K., Sames, B., Nasri, A., Piovesan, E. K., Elferhi, F., Skanji, A., Houla, Y., Soussi, M., & Wangreich, M. (2021). Ostracods as proxies for marginal marine to non-marine intervals in the mid-Cretaceous carbonate platform of the Central Tunisian Atlas (North Africa): Response to major short-term sea-level falls. *Cretaceous Research*, *117*, 104581. doi: 10.1016/j.cretres.2020.104581

Traverse, A. (2007). *Paleopalynology. Second edition*. Springer.

Vergés, J., Kullberg, J. C., Casas-Sainz, A., Vicente, G. D., Duarte, L. V., Fernández, M., Gómez, J. J., Gómez-Pugnaire, M. T., Jabaloy-Sánchez, A., López-Gómez, J., Macchiavely, C., Martín-Algarra, A., Martín-Chivelet, J., Muñoz, J. A., Quesada, C., Terrinha, P., Torné, M., & Vegas, R. (2019). An introduction to the Alpine Cycle in Iberia. In C. Quesada, & J. T. Oliveira (Eds.), *The Geology of Iberia: A Geodynamic Approach. Volume 3: The Alpine Cycle* (pp. 1–14). Springer Cham.

Villanueva-Amadoz, U., Sender L. M., Díez J. B., Ferrer J., & Pons D. (2011). Palynological studies of the boundary marls unit (Albian–Cenomanian) from northeastern Spain. Paleophytogeographical implications. *Geodiversitas*, *33*, 137–176. doi: 10.5252/g2011n1a7

Villanueva-Amadoz, U., Sender, L. M., Diez, J. B., Ferrer, J. J., & Pons, D. (2014). A new isoetalean microsporophyll from the latest Albian of northeastern Spain: Diversity in the development and dispersal strategies of microspores. *Acta Palaeontologica Polonica*, *59*(2), 479–490. doi: 10.4202/app.2012.0010

Wang, B., Shi, G., Xu, C., Spicer, R. A., Perrichot, V., Schmidt, A. R., Feldberg, K., Heinrichs, J., Chény, C., Pang, H., Liu, X., Gao, T., Wang, Z., Ślipiński, A., Solórzano-Kraemer, M. M., Heads, S. W., Thomas, M. J., Sadowski, E.-M., Szweso, J., Azar, D., Nel, A., Chen, J., Zhang, Qi, Zhang, Qin., Luo, C., Yu, T., Zheng, D., Zhang, H., & Engel, M. S. (2021). The mid-Miocene Zhangpu biota reveals an outstandingly rich rainforest biome in East Asia. *Science Advances*, *7*(18), eabg0625. doi: 10.1126/sciadv.abg0625

Wilkin, R. T., Barnes, H. L., & Brantley, S. L. (1996). The size distribution of framboidal pyrite in modern sediments: an indicator of redox conditions. *Geochimica et Cosmochimica Acta*, *60*(20), 3897–3912. doi: 10.1016/0016-7037(96)00209-8

Xing, L., Sames, B., McKellar, R. C., Xi, D., Bai, M., & Wan, X. (2018). A gigantic marine ostracod (Crustacea: Myodocopa) trapped in mid-Cretaceous Burmese amber. *Scientific Reports*, *8*(1), 1365. doi: 10.1038/s41598-018-19877-y

Yu, T., Thomson, U., Mu, L., Ross, A., Kennedy, J., Broly, P., Xia, F., Zhang, H., Wang, B., & Dilcher, D. (2019). An ammonite trapped in Burmese amber. *Proceedings of the National Academy of Sciences*, *116*(23), 11345–11350. doi: 10.1073/pnas.182129211

Supplementary information to:

Taphonomy and palaeoenvironmental interpretation of a new amber-bearing outcrop from the mid-Cretaceous of the Maestrazgo Basin (E Iberian Peninsula)

Sergio ÁLVAREZ-PARRA, Carlos A. BUENO-CEBOLLADA, Eduardo BARRÓN, Jordi PÉREZ-CANO, María Victoria PAREDES-ALIAGA, Cristóbal RUBIO, Ana RODRIGO, Nieves MELÉNDEZ, Xavier DELCLÒS, & Enrique PEÑALVER

Corresponding author: Sergio Álvarez-Parra (sergio.alvarez-parra@ub.edu)

Table S1

Taxa	Nº	%	Taxonomic affinity
Acritarcha			
Micrhystridium sp.	1	0.26	Acanthomorphitae
Dinoflagellata			
Canningia cf. *reticulata*	30	7.77	Areoligeraceae
Florentinia sp.	3	0.77	Gonyaulacaceae
Oligosphaeridium complex	97	25.13	Leptodinioideae
Palaeohystrichophora infusorioides	2	0.52	Peridiniaceae
Palaeohystrichophora sp.	1	0.26	Peridiniaceae
Palaeoperidinium spp.	16	4.14	Peridiniaceae
Spiniferites ramosus	7	1.81	Gonyaulacaceae
Spiniferites twistringiensis	3	0.77	Gonyaulacaceae
Tenua histrix	2	0.52	Gonyaulacaceae
Trichodinium castanea	1	0.26	Gonyaulacaceae
Undetermined dinocysts	60	15.54	-
Chlorophyta			
Cymathiosphaera sp.	1	0.26	Prasinophytina
Tasmanites sp.	1	0.26	Prasinophytina
Ovoidites sp.	1	0.26	Zygnemataceae
Lycophyta			
Camarozonosporites insignis	5	1.3	Lycopodiaceae
Camarozonosporites sp.	2	0.52	Lycopodiaceae
Monilophyta			
Appendicisporites cf. *crenimurus*	1	0.26	Anemiaceae
Appendicisporites sp.	1	0.26	Anemiaceae
Biretisporites potoniaei	1	0.26	Uncertain affinities
Cicatricosisporites venustus	1	0.26	Anemiaceae
Cicatricosisporites sp.	1	0.26	Anemiaceae
Crybelosporites pannuceus	2	0.52	Marsileaceae
Cyathidites australis	7	1.81	Uncertain affinities
Cyathidites minor	1	0.26	Uncertain affinities
Gleicheniidites senonicus	1	0.26	Gleicheniaceae
Granulatisporites sp.	1	0.26	Botryopteridales
Laevigatosporites spp.	2	0.52	Uncertain affinities
Microreticulatisporites sacalii	3	0.77	Botryopteridales
Osmundacidites wellmanii	2	0.52	Osmundaceae
Patellasporites tavaredensis	2	0.52	Uncertain affinities

Polypodiaceoisporites sp.	1	0.26	Polypodiaceae?
Undetermined trilete spores	10	2.59	-
Varirugosisporites sp.	1	0.26	Uncertain affinities
Gymnospermophyta			
Afropollis jardinus	2	0.52	Uncertain affinities
Araucariacites australis	37	9.58	Araucariaceae
Araucariacites spp.	6	1.56	Araucariaceae
Balmeiopsis limbata	9	2.33	Araucariaceae
Callialasporites dampieri	1	0.26	Araucariaceae
Classopollis major	18	4.66	Cheirolepidiaceae
Classopollis spp.	8	2.07	Cheirolepidiaceae
Inaperturopollenites dubius	5	1.3	Cupressaceae
Undetermined bisaccate pollen grains	23	5.96	-
Antophyta			
Dichastopollenites? sp.	2	0.52	Uncertain affinities
Tricolpites sp.	1	0.26	Eudicots
Undetermined pollen grains of angiosperms	1	0.26	-
Foraminifera			
Undetermined test lining	2	0.52	-
Total	386	100	

Table S1. Full list of palynomorphs from interval 11 of the La Dehesa locality (late Albian–early Cenomanian; Estercuel, Aragón, Spain), present in the palynological sample EMD-11.1.

Data S1–S4

Morphologies of pyrite crystals and framboids on microfossils and their EDX profiles, with the abundance of each element.

Data S1: Ostracod carapace *Cythereis* sp. Specimen MPZ 2024/31.

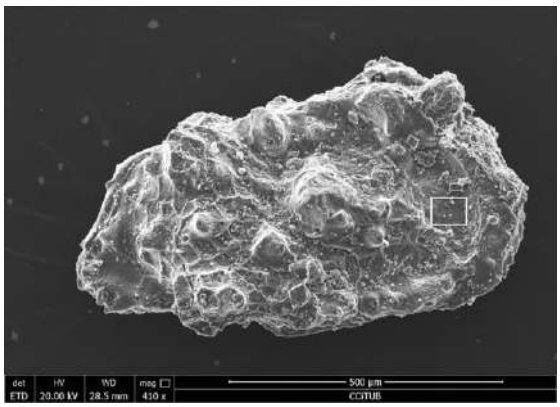

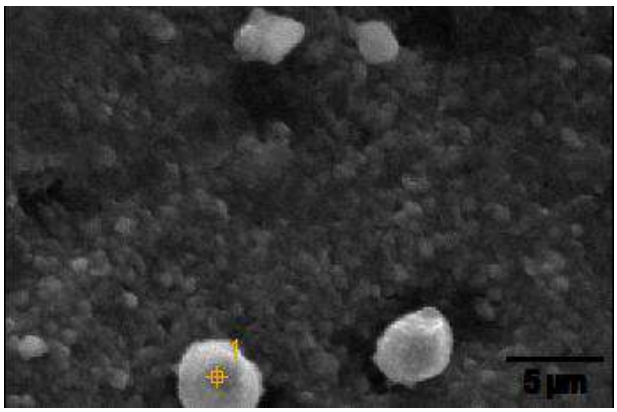

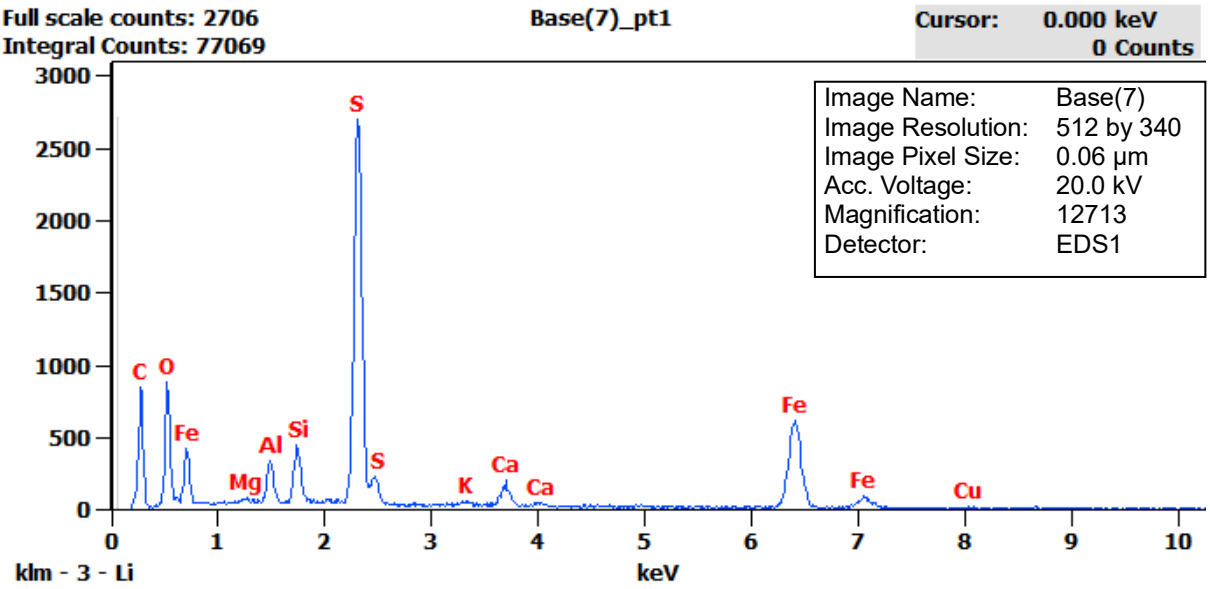

Weight %

	C	O	Mg	Al	Si	S	K	Ca	Fe	Cu
Base(7)_pt1	24.38	20.57	0.23	2.00	2.72	21.59	0.38	2.01	25.66	0.45

Atom %

	C	O	Mg	Al	Si	S	K	Ca	Fe	Cu
Base(7)_pt1	43.22	27.38	0.20	1.58	2.06	14.34	0.21	1.07	9.78	0.15

Compound %

	C	O	Mg	Al	Si	S	K	Ca	Fe	Cu
Base(7)_pt1	24.38	20.57	0.23	2.00	2.72	21.59	0.38	2.01	25.66	0.45

Data S2: Ostracod carapace of *Cythereis* (*Rehacythereis*) cf. *pseudobartensteini*. Specimen MPZ 2024/32.

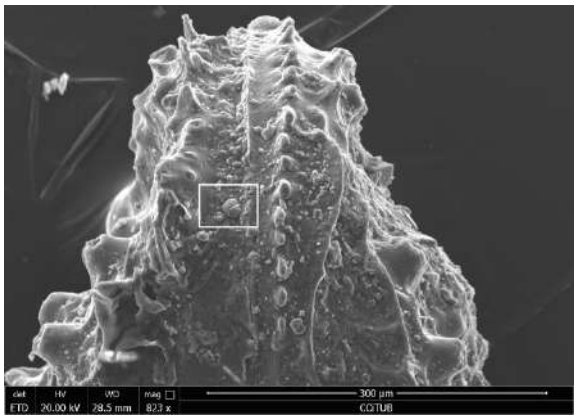

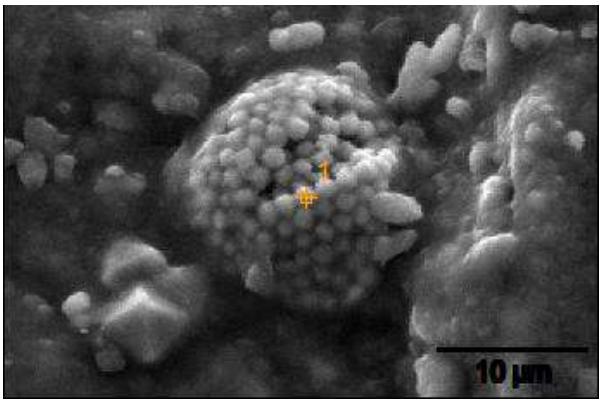

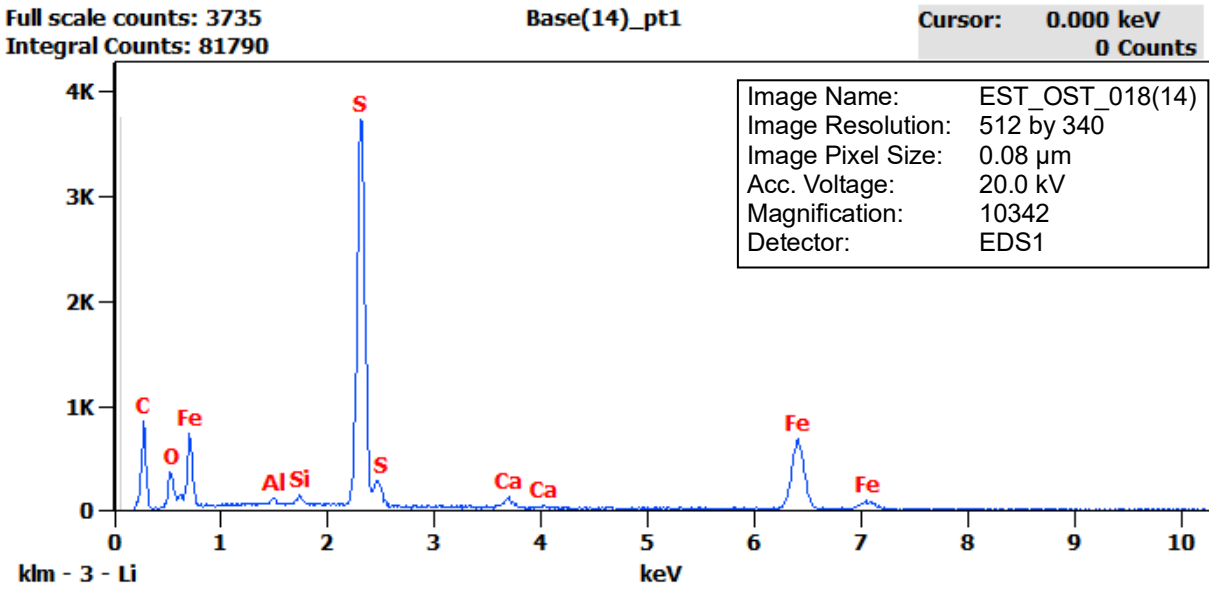

Weight %

	C	O	Al	Si	S	Ca	Fe
Base(14)_pt1	27.96	12.01	0.37	0.55	29.05	1.34	28.72

Atom %

	C	O	Al	Si	S	Ca	Fe
Base(14)_pt1	50.98	16.45	0.30	0.43	19.85	0.73	11.26

Compound %

	C	O	Al	Si	S	Ca	Fe
Base(14)_pt1	27.96	12.01	0.37	0.55	29.05	1.34	28.72

Data S3: Ostracod carapace of *Schuleridea* sp. Specimen MPZ 2024/45.

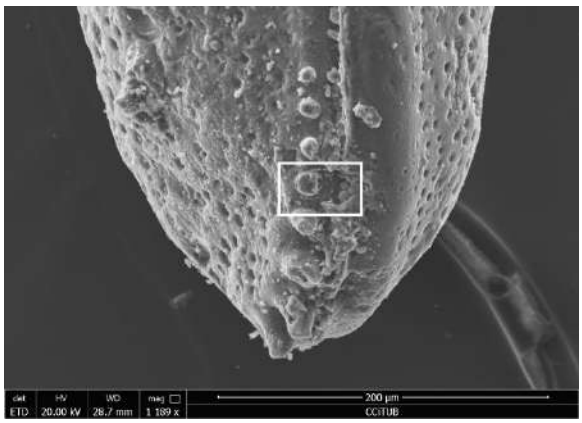

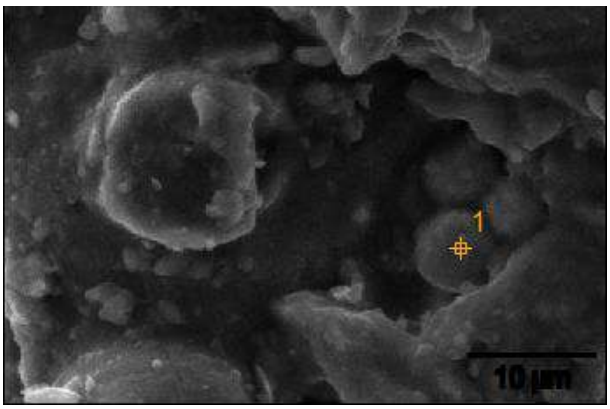

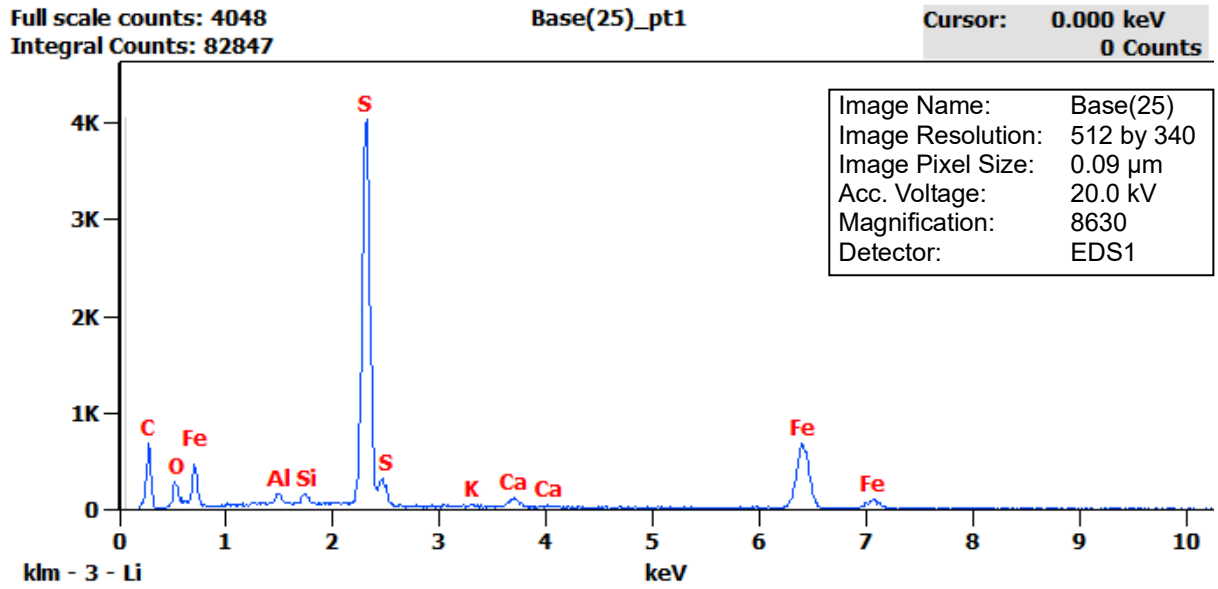

Weight %

	C	O	Al	Si	S	K	Ca	Fe
Base(25)_pt1	25.42	9.98	0.77	0.82	32.01	0.16	1.32	29.52

Atom %

	C	O	Al	Si	S	K	Ca	Fe
Base(25)_pt1	48.52	14.29	0.65	0.67	22.89	0.09	0.76	12.12

Compound %

	C	O	Al	Si	S	K	Ca	Fe
Base(25)_pt1	25.42	9.98	0.77	0.82	32.01	0.16	1.32	29.52

Data S4: Echinoid remain. Specimen MPZ 2024/25.

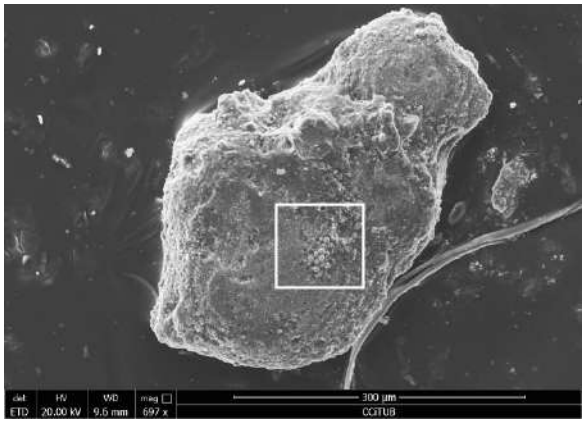

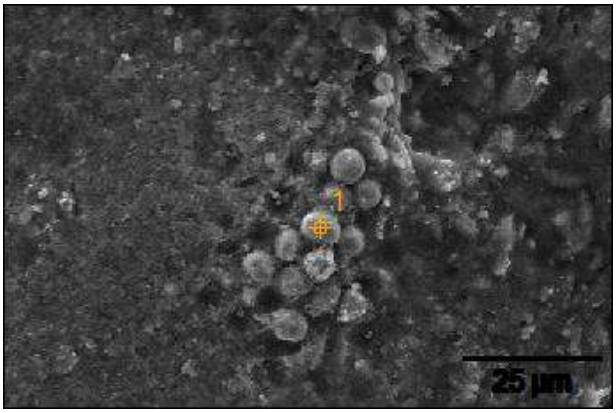

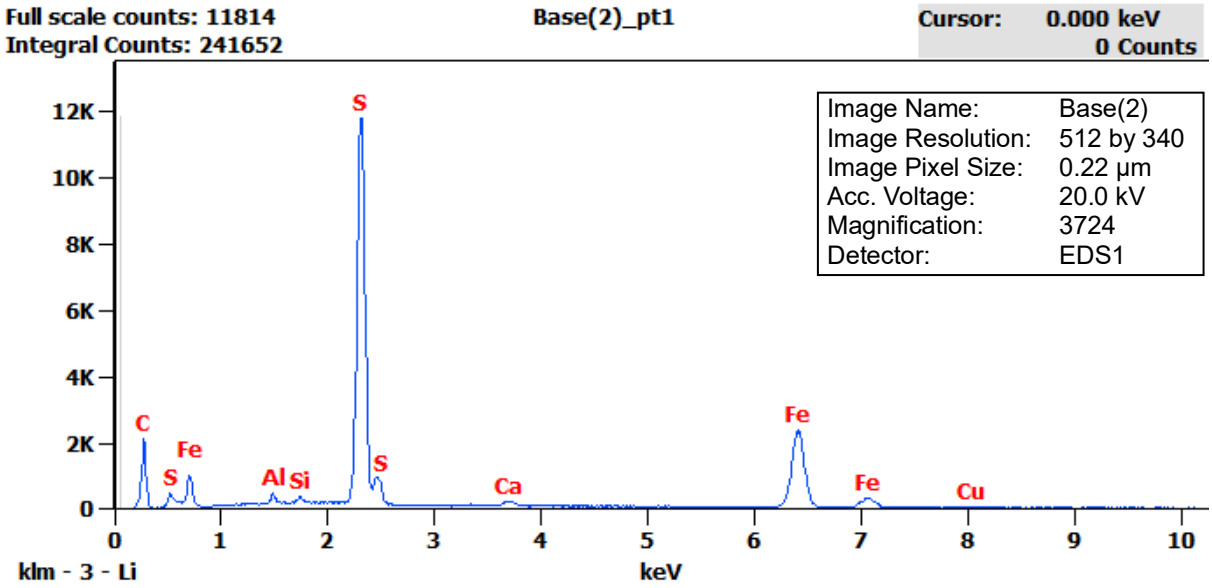

Weight %

	C	Al	Si	S	Ca	Fe	Cu
Base(2)_pt1	32.43	0.63	0.52	32.45	0.70	32.65	0.63

Atom %

	C	Al	Si	S	Ca	Fe	Cu
Base(2)_pt1	61.84	0.53	0.43	23.18	0.40	13.39	0.23

Compound %

	C	Al	Si	S	Ca	Fe	Cu
Base(2)_pt1	32.43	0.63	0.52	32.45	0.70	32.65	0.63